

Meta-learning For Few-Shot Time Series Crop Type Classification: A Benchmark On The EUROCROPSML Dataset

Joana Reuss^{a,*}, Jan Macdonald^d, Simon Becker^{d,e}, Konrad Schultka^d, Lorenz Richter^{d,f}, Marco Körner^{a,b,c}

^aTechnical University of Munich (TUM), TUM School of Engineering and Design, Department of Aerospace and Geodesy, Chair of Remote Sensing Technology, Munich, 80333, Germany

^bTechnical University of Munich (TUM), Munich Data Science Institute (MDSI), Garching, 85748, Germany

^cELLIS Unit Jena, University of Jena, Jena, Germany, Jena, 07743, Germany

^ddida Datenschmiede GmbH, Berlin, 10827, Germany

^eETH Zurich, Department of Mathematics, Zurich, 8004, Switzerland

^fZuse Institute Berlin, Berlin, 14195, Germany

Abstract

Spatial imbalances in crop type data pose significant challenges for accurate classification in remote sensing applications. Algorithms aiming at transferring knowledge from data-rich to data-scarce tasks have thus surged in popularity. However, despite their effectiveness in previous evaluations, their performance in challenging real-world applications is unclear and needs to be evaluated. This study benchmarks transfer learning and several meta-learning algorithms, including (*First-Order*) *Model-Agnostic Meta-Learning* ((FO)-MAML), *Almost No Inner Loop* (ANIL), and *Task-Informed Meta-Learning* (TIML), on the real-world EUROCROPSML time series dataset, which combines farmer-reported crop data with Sentinel-2 satellite observations from Estonia, Latvia, and Portugal. Our findings indicate that MAML-based meta-learning algorithms achieve slightly higher accuracy compared to simpler transfer learning methods when applied to crop type classification tasks in Estonia after pre-training on data from Latvia. However, this improvement comes at the cost of increased computational demands and training time. Moreover, we find that the transfer of knowledge between geographically disparate regions, such as Estonia and Portugal, poses significant challenges to all investigated algorithms. These insights underscore the trade-offs between accuracy and computational resource requirements in selecting machine learning methods for real-world crop type classification tasks and highlight the difficulties of transferring knowledge between different regions of the Earth. To facilitate future research in this domain, we present the first comprehensive benchmark for evaluating transfer and meta-learning methods for crop type classification under real-world conditions. The corresponding code is publicly available at <https://github.com/dida-do/eurocrops-meta-learning>.

Keywords: transfer learning; few-shot learning; meta-learning; crop type classification; time series classification; Sentinel-2.

1. Introduction

Satellites continuously generate spatio-temporal remote sensing data of the Earth's surface, which forms a cornerstone of modern *Earth observation* (EO) techniques. They play an important role in a very wide range of applications, from hurricane forecasting (Boussiou et al., 2022) or methane detection (Kumar et al., 2020) to vegetation analysis (Odenweller and Johnson, 1984; Reed et al., 1994). In particular, satellite imagery has been used in agriculture for fertilization analysis (Santaga et al., 2021), harvest detection (Marković et al., 2023), as well as yield forecast and crop assessment (Bekmukhamedov et al., 2024-01-16).

A common key challenge in these tasks is the efficient extraction of relevant and valuable information from the abundance of collected remote sensing data. Recently, *artificial intelligence* (AI) and particularly *machine learning* (ML) and *deep learning* (DL) methods have shown a significant impact on EO and remote sensing and can address these challenges across entire data processing chains (Tuia et al., 2025).

Crop data plays a vital role in supporting decision-making processes in various economic sectors related to food supply, agriculture, the environment, and forestry, as well as socio-economic development (Gómez et al., 2016). Analyzing and understanding the distribution of crop types in different regions is essential for making informed decisions about food security, infrastructure development, and agricultural management. Furthermore, variations in crop data are used directly in research on climate change (Song et al., 2021-06).

The availability of comprehensive crop data is crucial to fully leverage the potential benefits of data-driven ML methods. However, availability varies significantly across different geographical regions, reflecting a widespread Eurocentric and Amerocentric bias in spatio-temporal datasets (Shankar et al., 2017), which hinders the adoption of ML-based data processing in data-scarce regions until now.

Transfer and *meta-learning* ideas offer promising directions for overcoming such data imbalances. Transfer learning refers to the approach of generalizing insights obtained from one machine learning task (typically data-rich) to another related task (typically data-scarce) in order to improve the performance on

* Corresponding author.

E-Mail address: joana.reuss@tum.de (J. Reuss)

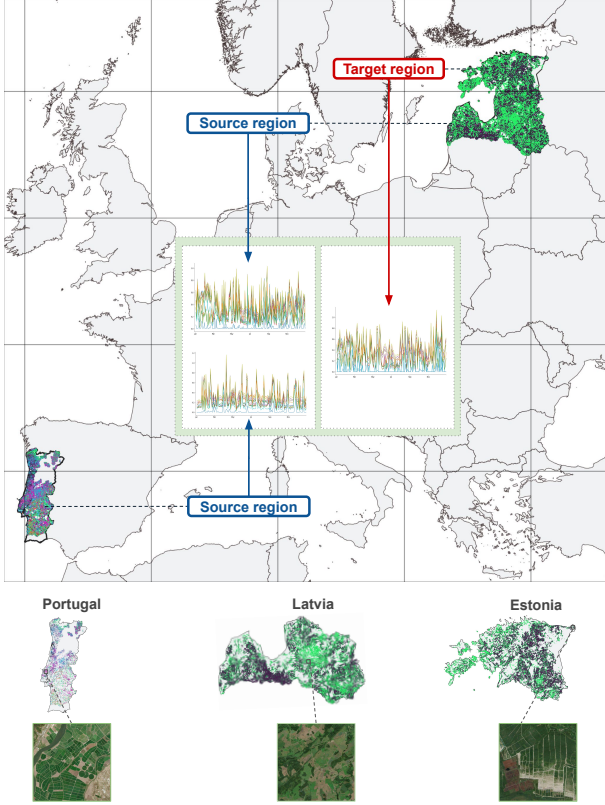


Figure 1: Visualization of crop fields (using EUROCROPS HCAT3 level 3 (Schneider et al., 2023a,b)) in the source and target region(s). The initial training is conducted on the Sentinel-2 L1C agricultural time series of the source region(s), followed by a process of fine-tuning and evaluation of the models on a distinct target region.

the second task. More broadly, meta-learning refers to methods that attempt to improve the generalization capabilities of machine learning models by considering multiple different but related tasks (each of which individually could be data-scarce). A general comparison of the two approaches was recently made by Dumoulin et al. (2021), see also Section 2 for more details.

Despite the growing interest in these approaches, there is currently a notable gap in the thorough analysis and comparison of various transfer learning and meta-learning techniques for multi-class crop type classification using spatio-temporal satellite data across multiple geographical regions. Moreover, the advantages and disadvantages of these techniques have not been thoroughly examined. In this work, we provide such an analysis. More precisely, we compare various existing ML approaches for time series crop type classification by benchmarking their cross-regional transfer performance on the EUROCROPSML dataset (Reuss et al., 2025). The dataset extends the EUROCROPS reference data (Schneider et al., 2021) with Sentinel-2 L1C reflectance data and is publicly available (Reuss and Macdonald, 2024). It is designed to resemble a real-world use case of data transfer across geographical regions for crop type classification algorithms intended for performing detailed benchmark analyses of various transfer learning and meta-learning algorithms.

In our benchmark study, we investigate how well different learning approaches transfer knowledge between crop classifica-

tion tasks using a state-of-the-art *Transformer* encoder architecture (Vaswani et al., 2017). Each approach is first trained on a source region and then evaluated on a different target region, as visualized in Figure 1. We examine the following approaches, detailed in Section 3:

Transfer Learning Transfer learning consists of a two-step procedure of pre-training an ML model that gets subsequently fine-tuned.

MAML The *Model-Agnostic Meta-Learning* approach introduced by Finn et al. (2017) and further investigated by Raghu et al. (2019-09-19); Ye and Chao (2021) is a very flexible and widely used optimization-based meta-learning algorithm (cf. Section 3.2.1).

FOMAML The *First-Order Model-Agnostic Meta-Learning* algorithm is a MAML variant with reduced computational costs proposed by Finn et al. (2017) (cf. Section 3.2.2).

ANIL The *Almost No Inner Loop* algorithm introduced by Raghu et al. (2019-09-19) is another computationally more efficient variant of MAML (cf. Section 3.2.3).

TIML The *Tasked-Informed Meta-Learning* algorithm was introduced by Tseng et al. (2022) and enriches MAML by including additional task-specific information (e.g., geographical coordinates) (cf. Section 3.2.4).

To establish a baseline, we also train a randomly initialized Transformer-based attention model directly on the target region data, allowing us to quantify the benefits of knowledge transfer through the above pre-training approaches.

In summary, our main findings comparing the aforementioned algorithms on the EUROCROPSML benchmark dataset are:

1. Meta-learning algorithms of the MAML family tend to slightly outperform the baseline and transfer learning algorithms (no pre-training & standard pre-training) as well as the algorithms of the TIML family in terms of prediction accuracy and Cohen’s kappa.
2. Despite having additional location information available, the algorithms of the TIML family show no improved performance.
3. The meta-learning algorithms tend to require longer overall training times and more computational resources compared to the baselines.
4. Meta-learning algorithms require more extensive tuning of hyperparameters, which has a detrimental effect on their marginally superior prediction performance.
5. Transferring pre-gained knowledge geographically poses a significant challenge for all investigated algorithms.

2. Related Work

Our study aims to have a realistic trial case to compare and benchmark existing and future crop type classification algorithms and their ability to generalize across different geographical regions. We start by reviewing different ML approaches commonly used for this task before discussing available crop datasets.

2.1. Transfer learning

The main idea of transfer learning is the transfer of knowledge from one task to another related task. This involves two phases. In the first phase, the ML model is trained on a (large) dataset associated with the first task (pre-training).

In the second phase, the pre-trained model is taken as an initialization for training on a (smaller) dataset associated with the second task (fine-tuning).

Transfer learning methods have been widely used to overcome the imbalance of agricultural data available in different parts of the world. For example, models to perform crop yield estimation demonstrated that extrapolating between different countries in South America showed promising results (Wang et al., 2018). Kerner et al. (2020) generated a cropland map for Togo in less than ten days by developing rapid transfer learning techniques for regions with little to no available ground truth data. Hao et al. (2020) trained a Random Forest-based crop type classification model on spatio-temporal Sentinel-2 data from areas in the United States and subsequently tested on regions in China and Canada. In general, transfer learning models showed promising capabilities in identifying crops, sometimes even without local training samples. Furthermore, it was noted that transfer learning techniques typically required longer time series data compared to instances where sufficient local data was utilized for crop type classification. Similarly, Antonijević et al. (2023) trained models to classify nine different types of crops in Brittany or Serbia while fine-tuning and testing them on data from the other respective area. They discovered that the transfer of knowledge from the original domain to the new was effective, both in terms of accuracy and computational efficiency.

2.2. Meta-learning

While transfer learning focuses on transferring knowledge and insights gained from one task to another related task, the core concept of meta-learning can be described as *learning-to-learn*.

In their seminal work, Thrun and Pratt (1998) introduce the concept of meta-learning as the task of learning properties of classes of functions from a few examples, that is, learning entire function spaces. On a less abstract level, the objective of meta-learning is to swiftly grasp a new task, a paradigm commonly referred to as *few-shot learning*. This typically involves adapting a machine learning model across several related tasks while monitoring the respective learning processes. The goal is then to improve the learning process itself to make a meta-learned model that is well suited for efficient adaptations to future tasks (Rusu et al., 2018; Yoon et al., 2018; Lee et al., 2019; Nichol et al., 2018). For a contemporary overview, see also the survey of Hospedales et al. (2022).

Adapted to our crop classification problem, meta-learning aims to learn about the process of crop classification itself so that it can generalize to new tasks, such as new regions or unseen crops, with minimal effort. On the other hand, transfer learning uses a pre-trained model and tries to adapt it to classify crops from an unknown region.

Meta-learning approaches can be divided into three groups:

Model-based These methods are based on fully trained cyclic or recurrent neural network models with internal or external memory that learn to adapt to their state by reading a short sequence of task-specific training data. Examples include *Memory-Augmented Neural Networks* (Santoro et al., 2016-06) and *Neural Attentive Meta-Learners* (Mishra et al., 2018).

Metric-based These approaches learn effective and task-adapted distance metrics that are combined with non-parametric techniques during inference. Examples of this include *Prototypical Networks* (Snell et al., 2017), *Matching Networks* (Vinyals et al., 2016), and *Relation Networks* (Sung et al., 2018).

Optimization-based These algorithms represent a major research direction within the area of meta-learning, focusing on the optimization process of training ML models across different tasks. By gaining insights into these learning processes, they enable for a joint optimization of, e.g., model hyperparameters and parameter initializations across tasks, allowing for a rapid adaptation to new tasks. The most prominent example is *Model-Agnostic Meta-Learning (MAML)* (Finn et al., 2017; Raghu et al., 2019-09-19; Ye and Chao, 2021).

In this work, we will focus on the third category, as it is most widely applicable and fairly independent of the chosen ML architecture.

2.3. Meta-learning in remote sensing

Remote sensing encompasses a wide range of problems, such as semantic segmentation (e.g., spatially resolved classifications of land cover types), change detection, and object detection. These often share underlying characteristic structures, making them suitable for meta-learning approaches (Schmitt et al., 2021). In fact, meta-learning has been successfully applied to geospatial data (Wang et al., 2020; Rußwurm et al., 2020; Tseng et al., 2021, 2022).

A distinctive feature of remote sensing and Earth observation applications is the association of most data with specific geographic locations. These, in turn, are inherently tied to the prevalence of predictive quantities, such as crop type categories. Hence, meta-learning methods can learn to take advantage of these prevalences by observing tasks from different locations.

More specifically, for crop type classification, there are three main reasons why the problem is predestined for meta-learning algorithms.

Seasonal variations Crop type classification often involves monitoring crop growth and phenology over time. Meta-learning approaches can learn to adapt to temporal variations in crop appearance and spectral characteristics (Wang et al., 2020), allowing a more robust classification in different growing seasons and agricultural cycles.

Source regions Remote sensing data is collected from various geographical regions. The dimension of the source region captures the variability in environmental conditions, terrain types, climate patterns, and land use dynamics. Classification models may need to adapt to differences in data distribution between regions, such as rice fields on steep mountain terraces versus flat wheat fields, or mixed cropping systems versus large-scale monoculture farming.

Sensor modalities Satellite data can be captured using different sensors, each with its own resolution, spectral bands, temporal frequency, and other characteristics (Sainte Fare Gar-not et al., 2020). Classification models may need to generalize across different sensor modalities while accounting for differences in data characteristics and noise patterns.

Explicitly addressing the second point, Tseng et al. (2022) introduced the *Task-Informed Meta-Learning (TIML)* algorithm to study crop type classification and yield estimation. It is a modification of the MAML algorithm (Finn et al., 2017) that incorporates prior location-dependent task information into the learned ML model. Tseng et al. (2022) found that the TIML algorithm performed best on average compared to four baseline methods on crop type classification tasks in three different countries (Brazil, Kenya, and Togo) based on the CROPHARVEST dataset (Tseng et al., 2021). In particular, TIML outperformed MAML in all the regions considered. The baselines considered by Tseng et al. (2022) were a randomly initialized classifier, a classifier pre-trained on the binary CROPHARVEST crop-vs.-non-crop identification task (cf. Section 2.5), a Random Forest model, and the MAML algorithm.

In another study, Rußwurm et al. (2020) observed that meta-learning algorithms can outperform regular pre-training of models on crop type data in a transfer learning setting when the dataset includes a distinct regional diversity. In the same work, they also found that meta-learning outperformed standard pre-training and randomly initialized baseline models without any pre-training when predicting crop types from heterogeneous sparse labels.

2.4. Benchmarking meta-learning algorithms

As meta-learning aims to train models to adapt quickly to new tasks with limited data by using prior knowledge from related tasks, it is not clear when it will perform better than standard transfer learning techniques, cf. Section 2.1.

For example, in the context of few-shot natural image classification Tian et al. (2020) have observed that transfer learning from a frozen pre-trained model by fine-tuning only the final classification layer of a neural network resulted in the best classification accuracy compared to various meta-learning algorithms.

In addition, Miranda et al. (2023) conducted experiments that compared both pre-training and meta-learning approaches to evaluate their effectiveness on various computer vision datasets as well as on the OpenWebText dataset (Gokaslan et al., 2019). They conclude that in instances where the diversity of a dataset is low, a pre-trained model generally outperforms the MAML algorithm. Conversely, in scenarios characterized by high formal diversity within a dataset, MAML tends to outperform a pre-trained model. Hence, there is a need to understand the diversity of the data structure for a given task to decide whether meta-learning algorithms could potentially perform better. It should be noted that Miranda et al. (2023) observed that the effect sizes that favor one approach over the other in the different regimes were generally considered small.

Furthermore, Triantafillou et al. (2020) remarked that meta-learning benchmarks lack in representing real-world use cases. They proposed a more realistic benchmark dataset META-DATASET to evaluate meta-learning algorithms on various classification tasks. By combining several previously publicly available existing datasets, they investigated the generalization to entirely new distributions.

This paper ties in with a better understanding of the performance of transfer learning and meta-learning algorithms on different data diversities specific to remote sensing and crop classification. It presents a benchmark on a real-world crop type dataset with different diversity levels, which allows an in-depth analysis of ML algorithms for Earth observation.

2.5. Crop datasets

Significant obstacles persist in the development of ML platforms that work with agricultural Earth observation data. This is primarily due to different labeling and classification standards, biases in regional coverage, and the scarcity of publicly available labeled data.

The novel dataset EUROCRPSML (Reuss and Macdonald, 2024; Reuss et al., 2025), based on EUROCRPS (Schneider et al., 2021, 2023b,a), overcomes this major hurdle by including international data that extends beyond political borders. This contrasts with national or regional datasets, such as the BREIZHCROPS dataset for Brittany (France) (Rußwurm et al., 2020) and the ZUERICROP dataset for the cantons Thurgau and Zurich (Switzerland) (Turkoglu et al., 2021), which provide detailed information only for very local areas.

Although there also exists a crop type classification CROPLAND DATA LAYER dataset published by the United States Department of Agriculture (National Agricultural Statistics Service, 2024), the labels provided only have an accuracy slightly above 80 %, directly affecting the usability for ML methods. This is not the case for the EUROCRPSML dataset, as it is based on the EUROCRPS labeling, which contains accurate data directly self-reported by the farmers themselves.

Finally, the CROPHARVEST collection (Tseng et al., 2021) is a global dataset consisting of 90 480 data points that unify 20 different smaller datasets containing crop type classification labels. The data is composed of Sentinel-2 top-of-atmosphere (L1C) observations, Sentinel-1 observations, ERA5 climatology

data, and topography data from a Digital Elevation Model (Tseng et al., 2021). However, most of those data points merely distinguish between crop vs. non-crop labels. Only 34.2 % of the data points contain additional agricultural class labels such as, *e.g.*, crop types. Furthermore, the types of crops in CROPHARVEST are generally grouped into only nine different classes (*cf.* Tseng et al., 2021, Figure 2b), namely cereals, vegetables and melons, fruits and nuts, oilseed crops, root/tuber crops, beverage and spice crops, leguminous crops, sugar crops, and other crops. This is in stark contrast to the granular resolution of the hierarchical and harmonized labeling scheme offered by EUROCRIPS (*cf.* Table 1). Moreover, each CROPHARVEST data point contains a yearly time series at monthly intervals, which results in a much lower temporal resolution compared to the EUROCRIPSML dataset with up to 216 time steps (*cf.* Section 1).

The diverse geographical coverage, the high number of data points and time steps, as well as the harmonized crop class scheme, were the determining factors in our selection of EUROCRIPSML as the dataset for our benchmarking experiments of real-world crop type classification.

3. Methodology

In this section, we describe the ML models and the different learning algorithms that are examined in our benchmark study using the EUROCRIPSML dataset.

3.1. Transformer model

For all experimental settings, *cf.* Section 4.3, we rely on a state-of-the-art Transformer encoder architecture with sinusoidal positional encoding (Vaswani et al., 2017; Schneider and Körner, 2021). We set the maximum sequence length of input data to 366 days (*i.e.*, a full year, including one leap day). This encoder model is combined with a single linear layer that maps Transformer encodings to the crop type class logits. Further details of this architecture are outlined in Appendix A.1.

We refer to the encoder part as the *backbone* of the model and denote it as

$$M_{\text{backbone}}[\theta_{\text{backbone}}] : \mathbb{R}^{n_b \times n_t} \rightarrow \mathbb{R}^{n_e},$$

where $n_b \in \mathbb{N}$ and $n_t \in \mathbb{N}$ denote the number of bands (channels) and time steps in the multispectral temporal input data, respectively, and $n_e \in \mathbb{N}$ denotes the Transformer embedding dimension. All trainable model parameters of the backbone are contained in the parameter vector θ_{backbone} . Similarly, we refer to the classification layer as *head* of the model and denote it as

$$M_{\text{head}}[\theta_{\text{head}}] : \mathbb{R}^{n_e} \rightarrow \mathbb{R}^{n_c},$$

where $n_c \in \mathbb{N}$ denotes the number of distinct classes. As before, θ_{head} collects all trainable model parameters of the classification head. Note that while the model backbone architecture remains unchanged for all our experiments, the number of classes and, thus, the classification head changes between different pre-training, fine-tuning, and meta-learning tasks.

The complete end-to-end model for a specific task is given by the composition

$$M[\theta] = M_{\text{head}}[\theta_{\text{head}}] \circ M_{\text{backbone}}[\theta_{\text{backbone}}],$$

where $\theta = [\theta_{\text{backbone}}, \theta_{\text{head}}]$ represents all trainable parameters from both the model backbone and head.

3.2. Meta-learning

Meta-learning, as introduced by Thrun and Pratt (1998), see also the recent overview of Huisman et al. (2021), aims to implement the concept of *learning-to-learn*. In other words, meta-learning uses a variety of smaller related tasks to extract general information about a learning process. The goal is to obtain a meta-learned model that is able to quickly adapt to new and unknown scenarios and, thus, can learn an unseen task fast and efficiently.

In the following, we focus on optimization-based meta-learning methods, which can be formulated as bi-level optimization problems consisting of nested *inner* and *outer* optimization loops.

To illustrate the main ideas, consider a distribution $p(\mathcal{T})$ over a set of related tasks $\mathcal{T} = \{\tau^{(1)}, \tau^{(2)}, \dots, \tau^{(N)}\}$, where each task $\tau^{(i)} = (\mathcal{D}_{\text{support}}^{(i)}, \mathcal{D}_{\text{query}}^{(i)}, \mathcal{L}^{(i)}) \in \mathcal{T}$ consists of a set of support (training) data points $\mathcal{D}_{\text{support}}^{(i)}$, a set of query (test) data points $\mathcal{D}_{\text{query}}^{(i)}$, and a loss function $\mathcal{L}^{(i)}$.

During *inner optimization*, we adapt a parametrized model $M[\theta]$ with learnable parameters θ on the support dataset by optimizing

$$\begin{aligned} \theta_{\text{opt}}^{(i)} &= \mathcal{A}(M, \mathcal{D}_{\text{support}}^{(i)}, \mathcal{L}^{(i)}, \omega) \\ &\approx \underset{\theta}{\text{argmin}} \mathcal{L}^{(i)}(M[\theta], \mathcal{D}_{\text{support}}^{(i)}), \end{aligned}$$

where \mathcal{A} is the chosen training algorithm, *e.g.*, mini-batch *stochastic gradient descent* (SGD). This algorithm depends on hyperparameters ω , such as the learning rate or the initialization θ_0 of the model parameters.

The resulting model can be evaluated for the task $\tau^{(i)}$ on the query dataset according to the corresponding loss function $\mathcal{L}^{(i)}(M[\theta_{\text{opt}}^{(i)}], \mathcal{D}_{\text{query}}^{(i)})$.

The goal of the *outer optimization* is then to improve these task evaluations by adapting the hyperparameters ω . The optimal values for all tasks are found by (approximately) identifying

$$\omega_{\text{opt}} = \underset{\omega}{\text{argmin}} \mathbb{E}_{\tau^{(i)} \sim p(\mathcal{T})} [\mathcal{L}_{\text{meta}}(\mathcal{A}(M, \mathcal{D}_{\text{support}}^{(i)}, \mathcal{L}^{(i)}, \omega), \mathcal{D}_{\text{query}}^{(i)})],$$

where $\mathcal{L}_{\text{meta}}$ is some suitable meta-learning loss function.

One common meta-learning framework is *n*-way *k*-shot *classification* (Hospedales et al., 2022), which instantiates a specific variant of few-shot learning. In this case, each of the task training sets $\mathcal{D}_{\text{support}}^{(i)}$ consists of $n \cdot k$ data points from n distinct classes (k data samples per class) and the same classification loss $\mathcal{L}^{(i)}$, *e.g.*, the softmax cross-entropy loss, is used for all tasks.

In our experiments, *cf.* Section 4.3, we follow this *n*-way *k*-shot setup. We use a softmax cross-entropy classification loss for the inner optimization over the support sets. For the meta objective $\mathcal{L}_{\text{meta}}$, we use an averaged evaluation softmax cross-entropy classification loss on the query sets.

3.2.1. MAML

Building on this general concept, a widely adopted meta-learning approach is *Model-Agnostic Meta-Learning* (MAML) (Finn et al., 2017). Specifically, it focuses on finding optimal initializations of the model that can quickly adapt to new tasks, measured by the number of training steps. In other words, the outer optimization over hyperparameters is restricted to the initialization of the model weights. Further, MAML relies on iterative gradient-based optimization methods, such as mini-batch SGD, for both the inner and the outer optimizations. Here, the number of adaptation steps s for inner optimization is chosen as a fixed, typically rather small, constant. The respective step sizes (learning rates) for the two optimization iterations are consequently referred to as the inner and outer learning rates.

The interplay between these learning rates is complex, making it challenging to find suitable combinations in the MAML algorithm. Different approaches addressing this include the choice of a very fine-grained separate learning rate for each task in the inner optimization (Li et al., 2017), adaptive learning of inner and outer learning rates (Singh Behl et al., 2019), as well as the training of a separate model to generate per-layer learning rates (Baik et al., 2020).

3.2.2. FOMAML

Due to the nested structure of the MAML bi-level optimization, obtaining gradients for the outer optimization involves the computation of second-order derivatives with respect to the model parameters. This comes with significant computational costs.

Discarding higher-order derivatives by setting them equal to zero, we arrive at a variation of MAML with reduced computational costs. This is called *First-Order Model-Agnostic Meta-Learning* (FOMAML) (Finn et al., 2017).

3.2.3. ANIL

The *Almost No Inner Loop* (ANIL) algorithm (Raghu et al., 2019-09-19) is another variation that streamlines the MAML algorithm in order to reduce its computational cost. This is achieved by restricting the inner optimization of MAML to only adapt the parameters θ_{head} associated with the classification head of the model while keeping the backbone parameters θ_{backbone} fixed.

This was motivated by the observations of Raghu et al. (2019-09-19) that for MAML, in many cases, the backbone parameters remained relatively stable across tasks. In their analysis for natural image classification tasks, the ANIL algorithm typically achieved a performance comparable to MAML.

3.2.4. TIML

The *Task-Informed Meta-Learning algorithm* (TIML) (Tseng et al., 2022) represents an extension of MAML. It incorporates task-specific information, such as geospatial locations of a region or parcel, in the form of cartesian coordinates. More precisely, given the geographic coordinates of a surface point $\mathbf{p}_{\text{polar}} = (\varphi, \lambda) \in \left[-\frac{\pi}{2}, \frac{\pi}{2}\right] \times [-\pi, \pi]$ represented by its spherical longitude

φ and latitude λ , spatial information is encoded by mapping it into a normalized three-dimensional Cartesian coordinate space

$$\mathbf{p}_{\text{cart}} = (\cos(\lambda) \cdot \cos(\varphi), \cos(\lambda) \cdot \sin(\varphi), \sin(\lambda))^T \in \mathbb{R}^3.$$

The original TIML algorithm only includes the spatial coordinates at the task level, more precisely, the central coordinates of the region or county associated with each task. Furthermore, Tseng et al. (2022) propose to add a one-shot encoded vector of ten higher-level crop categories to the task information. Thus, the task information remains constant within each individual task but changes across different tasks. We decided to make the following adjustments to TIML in our benchmark study:

1. We do not incorporate additional high-level information on crop categories since we replace the model head M_{head} to always exactly match the classes available in any task during each inner optimization. Hence, the model does not need more information on available crop categories.
2. We consider fine-grained spatial coordinates at the parcel level: We incorporate the coordinates of the centroid of each individual parcel present in a task instead of using the center of the county. The rationale behind this choice is that utilizing the location only at the county level can potentially result in spatial oversimplification. To illustrate, consider the case where a county exhibits an uneven distribution of crop classes, with certain crop type clusters in the North and others in the South. Incorporating the same location information to all parcels would fail to resolve these distinct clusters.

This leaves us with a unique 3-dimensional task information vector for each data point. This is either directly concatenated with the remaining time series (no encoder) or encoded into specific layers of the model architecture (encoder); see also Tseng et al. (2022) for details. For the latter, these encodings are treated as learnable model parameters during outer optimization. In accordance with the approach outlined in Tseng et al. (2022), we apply them once prior to the model backbone and once prior to the model head. In contrast to the model architecture originally considered by Tseng et al. (2022), we only use one layer for the classification head, while they allow multiple layers and apply the task encoding before each of them.

Additionally, when using the task encoder, we pad all input time series sequences to 366 days and mask out the padded values since the encoder requires fixed length input sequences. All remaining parameters can be obtained from Tseng et al. (2022).

Due to the less streamlined nature of the CROPHARVEST dataset considered by Tseng et al. (2022), the authors also employ a forgetful meta-learning routine. This is proposed to overcome the challenge that the majority of CROPHARVEST data points only allow for a binary classification into crop-vs.-non-crop categories, which creates a bias for meta-learning algorithms towards learning only this specific task. However, we skip the incorporation of forgetful meta-learning, since the nature of the EURO-CROPSML dataset already inherently provides room for extensive and diverse multi-class tasks.

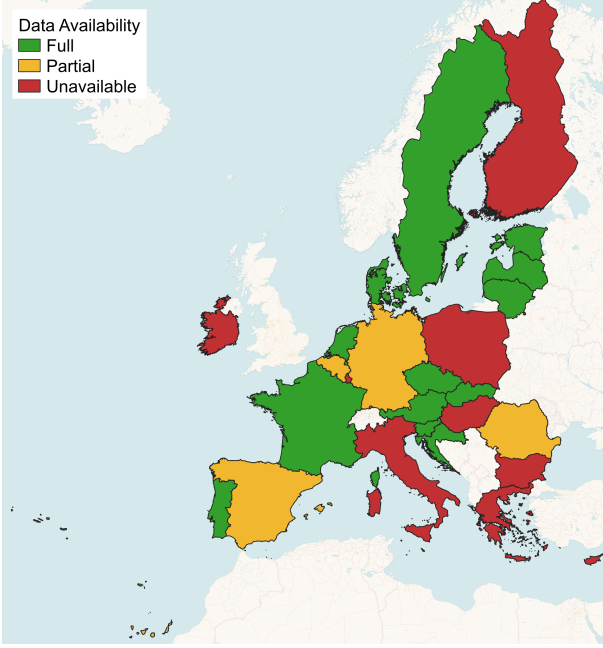


Figure 2: Currently 17 of the 27 member states of the European Union are harmonized within the EUROCRops dataset, with four states only offering partial data. The data availability refers to version 10 of the EUROCRops dataset (Schneider et al., 2023a).

4. Data and experiments

We present an extensive benchmark study analyzing different transfer learning and meta-learning algorithms on the EUROCRopsML (Reuss and Macdonald, 2024; Reuss et al., 2025) dataset, which is based on the previous EUROCRops (Schneider et al., 2023b) dataset. In the following, we give a brief overview of the dataset, summarizing the more detailed description of Reuss et al. (2025). Furthermore, we provide a comprehensive overview of the experimental setup employed in our benchmark study.

4.1. The EUROCRops dataset

EUROCRops is a reference dataset, introduced by Schneider et al. (2021), see also Schneider et al. (2023b) for details, containing pan-European agricultural parcel information data and crop types. Data have been collected directly from farmers’ self-declarations in accordance with the Common Agriculture Policy of the European Union. Hence, it provides a large collection of reliable, diverse, and unbiased reference data to develop and benchmark new ML methods and allows for in-depth investigation of agricultural activities.

Figure 2 shows an overview of the countries that comprise the full EUROCRops dataset. Table 1 provides a more detailed account of these data, showing the availability of data together with the number of crop classes, identified parcels, and available years of coverage.

To overcome country-specific class names and taxonomies for crop types, the dataset introduced the so-called *Hierarchical Crop and Agriculture Taxonomy (HCAT)* to harmonize pan-European standards (Schneider et al., 2023b).

Table 1: Member states of the EU sorted by the availability of their agricultural reference data. This refers to version 10 of the EUROCRops dataset (Schneider et al., 2023a). The *# crop classes* refers to the number of unique crop types after HCAT harmonization. The *# parcels* column refers to unique parcel geometries after removing potential duplicates.

†The data for Belgium, Germany, Romania, and Spain is incomplete, meaning only data for selected regions are available. No data is yet available for Bulgaria, Cyprus, Finland, Greece, Hungary, Ireland, Italy, Luxembourg, Malta, and Poland.

countries	# crop classes	# parcels	years
Austria	98	2 610 470	2021
Croatia	11	1 377 155	2020
Czechia	142	665 679	2023
Denmark	127	587 453	2019
Estonia	127	176 055	2021
France	149	9 517 878	2018
Latvia	103	431 174	2021
Lithuania	22	1 102 441	2021
Netherlands	141	766 645	2020
Portugal	79	100 000	2021
Slovakia	118	255 568	2021
Slovenia	99	824 449	2021
Sweden	48	1 210 533	2021
Belgium†	129	591 083	2021
Flanders	129	591 083	2021
Germany†	205	1 921 513	2021, 2023
Brandenburg	116	286 246	2023
Lower Saxony	150	902 441	2021
NRW	175	732 826	2021
Romania†	8	329 706	N/A
Border region	8	329 706	
Spain†	10	996 679	2021
Navarra	10	996 679	2021

4.2. The EUROCRopsML benchmarking dataset

EUROCRopsML (Reuss and Macdonald, 2024) is a time series dataset that combines the parcel information reference data and multi-class HCAT labels from EUROCRops with Sentinel-2 L1C optical satellite observations captured during the year 2021. Each parcel data point in EUROCRopsML contains an annual time series of cloud-free multi-spectral Sentinel-2 observation data, where each individual time step represents the median pixel value in the geometry of the parcel for each of the 13 Sentinel-2 spectral bands. In addition, the dataset contains further meta-data, including the spatial coordinates of the parcel’s centroid and Eurostat’s *GISCO Nomenclature of Territorial Units for Statistics (NUTS)* regions (Reuss et al., 2025).

Tailored specifically for evaluating (few-shot) crop type classification methodologies, this dataset encompasses agricultural data from three carefully selected European countries, providing a diverse and comprehensive resource for benchmarking ML algorithms within the agricultural domain.

4.2.1. Study area

The EUROCRopsML dataset provides data for three European countries as *regions of interest (ROI)*: **Estonia**, **Latvia**, and **Portugal**, as shown in Figure 1.

Estonia and Latvia provide a suitable context for investigating the impact of similarities between two neighboring countries during the processes of knowledge transfer learning and meta-learning. Furthermore, adding data from Portugal allows us to examine the influence of different climate conditions, cultivation practices, and prevalence of crop classes when transferring

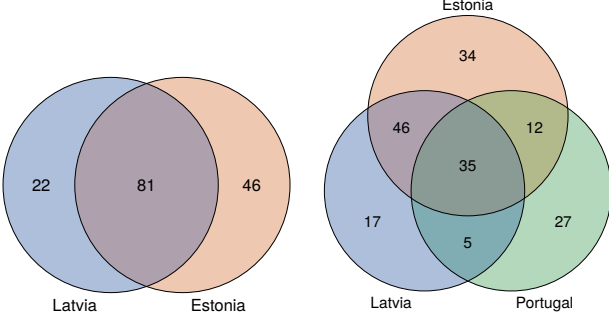


Figure 3: The number of annotated crop classes that are shared and distinct between the three ROIs: Estonia, Latvia, and Portugal.

Table 2: The number of data points and distinct crop classes for the three countries that comprise the EUROCRPSML dataset. The number of data points refers to the number of unique parcels after pre-processing.

country	# data points	# crop classes
Estonia	175 906	127
Latvia	431 143	103
Portugal	99 634	79

knowledge gained from one region to a remote region. This becomes particularly interesting when the geographic location of parcels is explicitly taken into account by ML models and algorithms, *e.g.*, TIML, since the Baltic states and Portugal share crop class occurrences, as illustrated in Figure 3, with very distant geographic locations.

The details of the dataset are shown in Table 2. It consists of a total of 706 683 multi-class labeled data points with a total of 176 distinct classes, 35 of which are common to the three ROI countries, *cf.* Figure 3.

The map in Figure 4 shows the spatial distribution of crop classes for Estonia, Latvia, and Portugal, clearly demonstrating significant differences. For further illustrations of the different cultivation practices within the EUROCRPSML countries, see Reuss et al. (2025, Figures 1-3).

Within our benchmark study, we consider the following two scenarios for transfer learning and meta-learning, previously defined in Reuss et al. (2025):

Latvia→Estonia (LV→EE) The models are pre-trained on Latvian data and subsequently fine-tuned and evaluated on Estonian data. The pre-training dataset contains 103 distinct classes. During fine-tuning, the models see 127 classes in total, out of which 46 were not previously seen during pre-training.

Latvia+Portugal→Estonia (LV+PT→EE) The pre-training is conducted on data from Latvia and Portugal with a total of 142 classes, followed by fine-tuning and evaluating on data from Estonia. The fine-tuning dataset contains 127 distinct classes, of which 34 were not previously seen during pre-training.

4.2.2. Crop classes

The original composition of the dataset, the abundance of different crop classes, and the distribution of crop classes seen

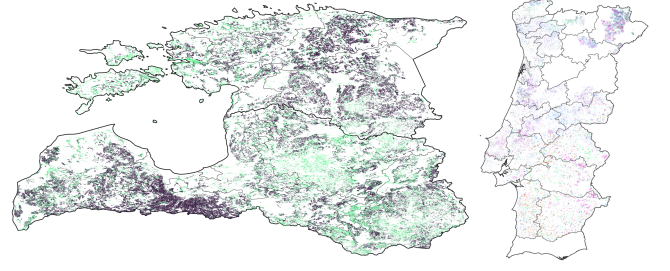


Figure 4: Illustration of the distribution of crop type labels for Estonia and Latvia (left) and Portugal (right), using EUROCRPS HCAT3 level 3 (Schneider et al., 2023a,b). The differences in the density of available data are clearly visible.

and unseen during the fine-tuning stage are illustrated in Figure 5. The pasture meadow grassland grass class is the predominant class in Latvia (215 026 of 431 143 parcels) and Estonia (84 104 of 175 906 parcels) and the third most frequent class in Portugal (16 475 of 99 634 parcels). Hence, for the pre-training stage, we resample it to the median frequency of all other classes. Figure 5 (bottom) shows that the percentage of total data points during fine-tuning that were not seen during pre-training on data from Latvia is roughly 10 %. When data from Portugal are added, that number reduces to roughly 2 %.

4.2.3. Splits

For the pre-training stage, the pre-built data splits allocate 80 % of the data to the training set and reserve the remaining 20 % for validation and hyperparameter tuning. The first use case (LV→EE) yields 172 993 samples in the training subset and 43 249 samples in the validation subset. For the second use case (LV+PT→EE), the training subset consists of 239 538 data points, while 59 885 are used for validation.

For the fine-tuning stage, the predefined splits reserve 60 % of Estonia’s data for training (105 543 samples) and 20% for validation and testing, respectively. From the complete validation set, only 1000 fixed final data points are sampled; whereas, for testing, all 35 182 samples are kept.

4.3. Experimental setup

From the pre-processed EUROCRPSML data, we keep all 13 Sentinel-2 spectral bands except band B10 (cirrus SWIR), which is typically used for cloud detection. This band is not further necessary here since the data EUROCRPSML pre-processing pipeline of Reuss et al. (2025) already performs cloud removal.

For both use cases outlined in Section 4.2.1, we compare regular transfer learning and four meta-learning algorithms (*i.e.*, MAML, FOMAML, ANIL, TIML) for training the same Transformer model on the corresponding pre-training dataset and then fine-tune each model on the Estonia data. In addition, we also consider training a randomly initialized Transformer model from scratch without any pre-training on the same fine-tuning tasks as a baseline comparison.

4.3.1. Pre-training setup

We use all training data for the transfer learning baseline to pre-train the Transformer model and validate it on the validation

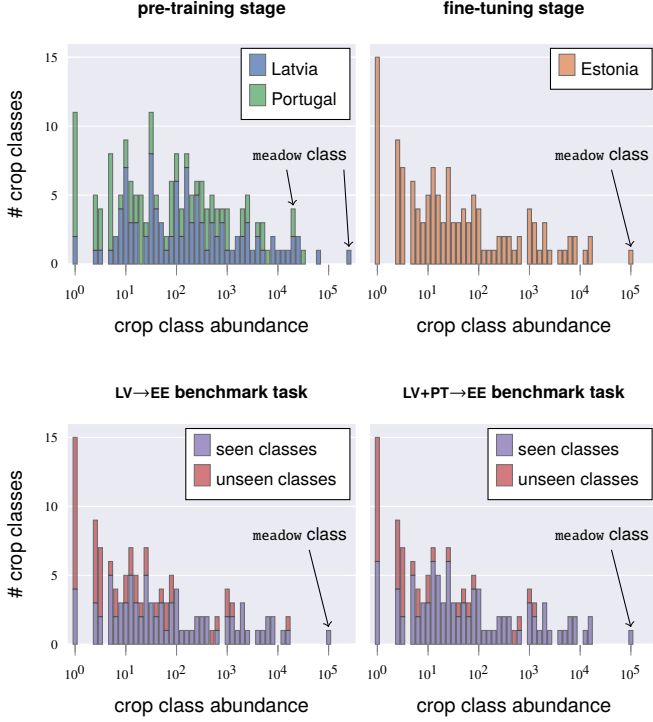


Figure 5: **Top:** Histograms showing the (stacked) binned distribution of the number of crop classes of a certain abundance (# of parcels of that class) (in a log scale) in both the pre-training and fine-tuning datasets.

Bottom: Histograms showing the stacked binned distribution of the number of crop classes in the fine-tuning data from Estonia of a certain abundance (# of samples of that class) (in a log scale) that were previously seen or unseen during the pre-training on either the data from Latvia only or data from Latvia and Portugal.

data. In order to identify the optimal setting for transfer learning, we consider batch size and cosine annealing as additional hyperparameters to the learning rate. The detailed configuration can be found in [Appendix A.4](#).

For meta-learning algorithms, we further sample meta-training and meta-validation tasks $\tau \in \mathcal{T}$ following the n -way k -shot paradigm for few-shot learning as follows:

Step 1: Sampling a NUTS-region With a probability given by the ratio of the number of data points per region to the total number of data points, we sample one of the regions LV003, LV005, LV006, LV007, LV008, LV009, PT11, PT15, PT16, PT17, and PT18, where the Portuguese regions (PT) are only considered for the second use case (LV+PT→EE) mentioned above. For Latvia (LV) the regions correspond to the country’s NUTS level-3 regions. For Portugal (PT) they reflect NUTS level-2 regions, as the Portuguese NUTS level-3 regions are relatively small and would hinder the creation of meaningful meta-learning tasks. A visualization of the NUTS regions can be seen in [Figure 6](#).

Step 2: Sampling a task We uniformly sample n random distinct classes that are present in the previously selected region. For each class, we then uniformly sample k_{query} random data points for the query set $\mathcal{D}_{\text{query}}$. Similarly, from the remaining samples, for each of the n classes,

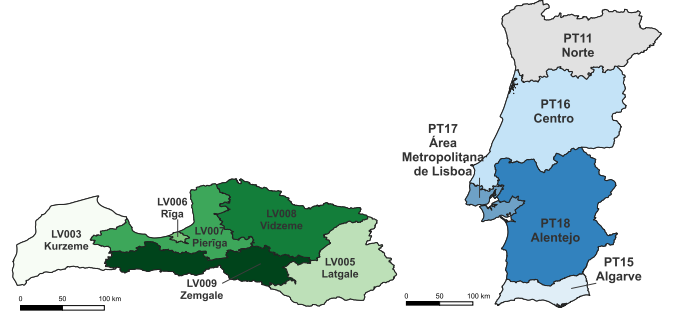


Figure 6: NUTS regions for Latvia (left) and Portugal (right) used for sampling meta-learning tasks.

we uniformly select k_{support} random data points for the support set $\mathcal{D}_{\text{support}}$ of the task. If after sampling the query set, there are only fewer than k_{support} data points left for sampling from a specific class, then we include all of them in the support set.

Experiments are conducted for $n \in \{4, 10\}$ and $k \in \{1, 10\}$. For all meta-learning algorithms and n -way k -shot settings, we consider the simplest algorithm variant with one gradient step (i.e., $s = 1$) in the inner optimization. For the setting $n = 4$ and $k = 1$, we also consider variants with multiple inner gradient steps $s \in \{1, 4, 10\}$. A more detailed outline and analysis of the meta-learning settings can be found in [Appendix A.3](#).

During meta-learning, we sample a fixed set of 100 meta-validation tasks for model validation and hyperparameter tuning, cf. [Appendix A.2](#), from the pre-training validation subset following steps 1 and 2 so that model validation is always performed on the same set of tasks.

In order to assess the ability of different transfer and meta-learning algorithms to cope with data-scarce situations, we fine-tune the models in various few-shot settings with 1, 5, 10, 20, 100, 200, or 500 shots (cf. [Reuss et al. \(2025\)](#)).

4.3.2. Fine-tuning setup

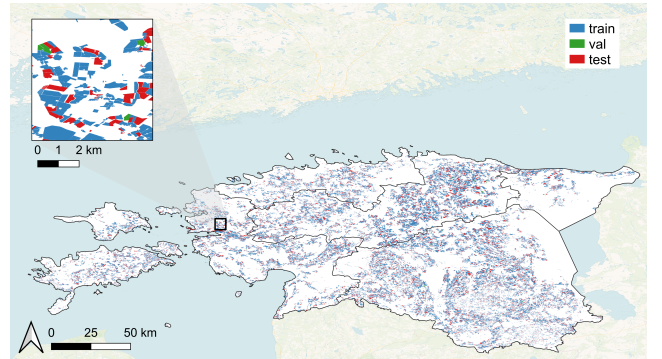


Figure 7: Spatial distribution of the fine-tuning dataset. The entire Estonia data is randomly split into train (60 %), validation (20 %), and test (20 %). For the final validation set, only 1000 samples are used. As can be seen in the map, the distribution of the data is spatially uniform throughout the country.

In addition, we train the baseline on all of the training data

from Estonia to quantify the complexity of the downstream task in a non-few-shot setting. We use the 1000 fixed data points sampled from the validation subset for model validation and hyperparameter tuning and finally evaluate the fully trained model on the complete 35 182 samples from the test subset. In order to evaluate the robustness of the results and reproducibility of the algorithms’ performances, we conduct all experiments five times, repeated with different random seeds (influencing, e.g., random parameter initialization and mini-batch sampling, cf. Appendix A.5).

Figure 7 visualizes the spatial distribution of the fine-tuning dataset, including all training samples.

5. Results

We present the best results for each algorithm and fine-tuning task in this section and defer a detailed analysis of algorithm variations and hyperparameter influences to Appendix A.2. The tables in this section compare the randomly initialized baseline model (no pre-training) to transfer learning, and the meta-learning algorithms ANIL, MAML, FOMAML, and TIML (with and without encoder). In each case, we report the mean and standard deviation estimated from the repeated experiments with varying random seeds, as detailed in Section 4.3.2 and Appendix A.5.

The overall classification accuracy (normalized by all instances) a_{OA} served as the main validation metric in our experiments. However, for data suffering from a class imbalance, this metric can be dominated by the majority classes and less sensitive to minority classes. Hence, the final models were additionally evaluated using Cohen’s kappa coefficient κ , which takes into account the imbalances in the underlying label distribution (Wang et al., 2020).

When training the randomly initialized baseline model on the full training data of the fine-tuning task, we received a final accuracy of $a_{OA} = 0.787 \pm 0.004$ and a final Cohen’s kappa score of $\kappa = 0.705 \pm 0.002$ on the test set. This can serve as a general reference value for the overall difficulty of the learning task on the Estonian data.

Table 3a ($LV \rightarrow EE$) and Table 3b ($LV+PT \rightarrow EE$) highlight the results when fine-tuning various pre-trained models on the data from Estonia. For $LV \rightarrow EE$ the standard transfer learning approach did not lead to any improvement in precision, compared to not pre-training at all. Algorithms belonging to the MAML family (i.e., ANIL, (FO-)MAML) tend to perform better as the number of fine-tuning shots increases (e.g., MAML reached $a_{OA} \approx 65\%$ accuracy for the 500-shot benchmark task). Furthermore, TIML (without an encoder) shows comparable results. In contrast, the encoder version of TIML achieves the highest classification accuracy for the extremely data-scarce 1-shot benchmark task, outperforming alternative approaches by a significant margin. However, this approach performs poorly for tasks with 100 shots and higher. Compared to Table 3a, Table 3b shows that the incorporation of additional data from Portugal during pre-training did not lead to improvements during fine-tuning. This becomes quite apparent when looking at the randomly initialized baseline model without pre-training that is not exposed to any

data from Portugal and outperforms all other algorithms for the 1-, 5-, 10- and 20-shot benchmark tasks.

Table 4a ($LV \rightarrow EE$) and Table 4b ($LV+PT \rightarrow EE$) provide additional insights into a more comprehensive analysis considering subsets of classes that are shared or not shared between pre-training and fine-tuning countries. They demonstrate the dominance of the meadow class in the learned data. For the overlapping classes ($EE \cap LV$) in the learning task $LV \rightarrow EE$, the MAML algorithm performed the best (cf. Table 4a). For the learning task that involves Portugal data (cf. Table 4b), the accuracy tends to be generally lower. The few-shot performance of all algorithms is significantly lower when evaluated on those classes not previously seen during pre-training ($EE \setminus (LV \cup PT)$).

6. Discussion

6.1. Overall performance and impact of pre-training

Our results show nuanced patterns in the effectiveness of different approaches for knowledge transfer across geographical regions. Although the results in Tables 3a and 3b show that there is no single algorithm that consistently outperforms the others in all scenarios, meta-learning approaches demonstrate particular strengths in specific tasks.

6.1.1. Effect of pre-training on data from Latvia

Table 3a ($LV \rightarrow EE$) highlights the benchmark results for transferring knowledge gained from Latvian data to Estonian data. The findings suggest that meta-learning algorithms, particularly those of the MAML family, exhibit a marginal superiority in prediction accuracy compared to the baseline without any pre-training and standard transfer learning. This is further validated by Cohen’s kappa, which also exhibits the highest values for algorithms of the MAML family. In contrast, despite demonstrating relatively strong accuracy in low ($k \leq 20$) few-shot tasks, the randomly initialized baseline model achieves a rather low Cohen’s kappa score. This suggests that it may have mainly learned to predict the dominant crop class pasture meadow grassland grass, instead of effectively learning the distinctions between the various crop classes, as is confirmed by the results shown in Tables 3a and 3b.

The relative importance of the pasture meadow grassland grass class becomes clearer when analyzing the 20-shot scenario regarding the classification accuracy while removing the pasture meadow grassland grass class (cf. Table 4a (20-shot $LV \rightarrow EE$)). It clearly shows a significant drop in accuracy for all algorithms when the pasture meadow grassland grass class is removed ($(EE \cap LV) \setminus (\text{pasture meadow grassland grass})$). The most dramatic drop is seen for the baseline model without pre-training, followed by TIML (with encoder). This again confirms the inferiority of TIML’s Cohen’s kappa as mentioned earlier. Moreover, as visualized in Figure 3, some crop type classes are shared between Latvia, Portugal, and Estonia, while others are not. Hence, it is of interest to ascertain whether, during the process of fine-tuning, the models demonstrate enhanced performance on those classes that were already encountered during the pre-training phase. Table 4a examines the performance on classes that overlap between Latvia and Estonia ($EE \cap LV$) and on those that do not ($EE \setminus LV$).

Table 3: Results for the different benchmark task. The metrics *classification accuracy* and *Cohen’s kappa coefficient* were evaluated on the test dataset for the best performing pre-training scenario (in terms of accuracy on the validation dataset) per algorithm and few-shot task. We report the mean \pm standard deviation over five repeated experimental runs in all cases. Cases in which the **LV+PT**→**EE** was an improvement over the corresponding **LV**→**EE** result in Table 3a are color highlighted. The best result per task and metric is marked in **bold**.

[‡] The results of the baseline algorithm with no pre-training are independent of the benchmark scenario and thus identical in Table 3a and Table 3b.

(a) Results for the **LV**→**EE** benchmark task.

benchmark task (k -shot)		1	5	10	20	100	200	500
algorithm								
accuracy	no pre-training [‡]	0.17 \pm 0.14	0.33 \pm 0.11	0.438 \pm 0.027	0.490 \pm 0.020	0.518 \pm 0.033	0.573 \pm 0.019	0.6317 \pm 0.0062
	transfer learning	0.143 \pm 0.070	0.203 \pm 0.081	0.254 \pm 0.060	0.365 \pm 0.081	0.464 \pm 0.042	0.503 \pm 0.032	0.575 \pm 0.048
	ANIL	0.189 \pm 0.047	0.250 \pm 0.076	0.419 \pm 0.045	0.490 \pm 0.069	0.561 \pm 0.034	0.589 \pm 0.020	0.652 \pm 0.011
	MAML	0.176 \pm 0.077	0.259 \pm 0.088	0.390 \pm 0.035	0.507 \pm 0.057	0.552 \pm 0.023	0.611 \pm 0.043	0.648 \pm 0.017
	FOMAML	0.21 \pm 0.11	0.228 \pm 0.052	0.416 \pm 0.047	0.476 \pm 0.039	0.516 \pm 0.036	0.557 \pm 0.018	0.6191 \pm 0.0069
	TIML (encoder)	0.247 \pm 0.092	0.25 \pm 0.11	0.368 \pm 0.040	0.423 \pm 0.067	0.494 \pm 0.045	0.517 \pm 0.022	0.591 \pm 0.021
	TIML (no encoder)	0.18 \pm 0.12	0.26 \pm 0.10	0.337 \pm 0.069	0.456 \pm 0.058	0.530 \pm 0.044	0.535 \pm 0.018	0.637 \pm 0.010
Cohen's kappa	no pre-training [‡]	0.004 \pm 0.033	0.094 \pm 0.035	0.206 \pm 0.047	0.25 \pm 0.13	0.367 \pm 0.058	0.466 \pm 0.018	0.5292 \pm 0.0041
	transfer learning	0.079 \pm 0.043	0.124 \pm 0.059	0.165 \pm 0.079	0.266 \pm 0.072	0.361 \pm 0.053	0.399 \pm 0.038	0.482 \pm 0.053
	ANIL	0.073 \pm 0.079	0.156 \pm 0.020	0.22 \pm 0.13	0.358 \pm 0.040	0.421 \pm 0.040	0.476 \pm 0.028	0.556 \pm 0.010
	MAML	0.106 \pm 0.032	0.119 \pm 0.029	0.272 \pm 0.021	0.362 \pm 0.050	0.406 \pm 0.030	0.479 \pm 0.056	0.534 \pm 0.034
	FOMAML	0.069 \pm 0.068	0.120 \pm 0.028	0.224 \pm 0.042	0.298 \pm 0.051	0.383 \pm 0.039	0.449 \pm 0.016	0.5102 \pm 0.0073
	TIML (encoder)	0.113 \pm 0.072	0.139 \pm 0.043	0.189 \pm 0.039	0.266 \pm 0.036	0.358 \pm 0.029	0.370 \pm 0.033	0.476 \pm 0.019
	TIML (no encoder)	0.107 \pm 0.052	0.180 \pm 0.043	0.219 \pm 0.024	0.314 \pm 0.046	0.406 \pm 0.026	0.425 \pm 0.018	0.5393 \pm 0.0064

(b) Results for the **LV+PT**→**EE** benchmark task.

benchmark task (k -shot)		1	5	10	20	100	200	500
algorithm								
accuracy	no pre-training [‡]	0.17 ± 0.14	0.33 ± 0.11	0.438 ± 0.027	0.490 ± 0.020	0.518 ± 0.033	0.573 ± 0.019	0.6317 ± 0.0062
	transfer learning	0.0787 ± 0.0091	0.1233 ± 0.0058	0.249 ± 0.098	0.292 ± 0.089	0.405 ± 0.023	0.473 ± 0.033	0.583 ± 0.028
	ANIL	0.154 ± 0.050	0.200 ± 0.020	0.321 ± 0.090	0.480 ± 0.045	0.538 ± 0.028	0.5761 ± 0.0098	0.623 ± 0.019
	MAML	0.117 ± 0.013	0.183 ± 0.018	0.366 ± 0.086	0.452 ± 0.094	0.517 ± 0.016	0.568 ± 0.017	0.637 ± 0.014
	FOMAML	0.103 ± 0.011	0.192 ± 0.035	0.33 ± 0.10	0.445 ± 0.058	0.512 ± 0.014	0.562 ± 0.028	0.623 ± 0.011
	TIML (encoder)	0.128 ± 0.031	0.163 ± 0.031	0.344 ± 0.084	0.438 ± 0.031	0.488 ± 0.029	0.473 ± 0.038	0.587 ± 0.024
	TIML (no encoder)	0.162 ± 0.074	0.189 ± 0.027	0.299 ± 0.018	0.441 ± 0.070	0.516 ± 0.063	0.538 ± 0.021	0.622 ± 0.012
Cohen's kappa	no pre-training [‡]	0.004 ± 0.033	0.094 ± 0.035	0.206 ± 0.047	0.25 ± 0.13	0.367 ± 0.058	0.466 ± 0.018	0.5292 ± 0.0041
	transfer learning	0.0657 ± 0.0079	0.1093 ± 0.0074	0.173 ± 0.055	0.208 ± 0.061	0.298 ± 0.037	0.379 ± 0.030	0.481 ± 0.027
	ANIL	0.1090 ± 0.0080	0.1547 ± 0.0092	0.215 ± 0.069	0.330 ± 0.034	0.396 ± 0.027	0.461 ± 0.019	0.519 ± 0.025
	MAML	0.084 ± 0.045	0.140 ± 0.012	0.231 ± 0.064	0.320 ± 0.065	0.386 ± 0.028	0.458 ± 0.021	0.537 ± 0.015
	FOMAML	0.082 ± 0.026	0.133 ± 0.023	0.197 ± 0.049	0.317 ± 0.042	0.381 ± 0.020	0.457 ± 0.025	0.522 ± 0.012
	TIML (encoder)	0.068 ± 0.026	0.094 ± 0.021	0.148 ± 0.086	0.230 ± 0.088	0.332 ± 0.016	0.340 ± 0.016	0.459 ± 0.039
	TIML (no encoder)	0.102 ± 0.023	0.137 ± 0.022	0.205 ± 0.017	0.316 ± 0.047	0.403 ± 0.047	0.432 ± 0.020	0.525 ± 0.011

In general, meta-learning approaches outperform other methods. MAML, in particular, demonstrates strong performance for overlapping classes ($EE \cap LV$), suggesting that meta-learning provides a significant advantage for previously encountered classes. Most pre-training algorithms (except FOMAML) even maintained better accuracy on classes exclusively present within Estonia ($EE \setminus LV$) compared to the baseline. This indicates that some generally learned features of the model backbone are also valuable for adapting to those new classes. This effect is most pronounced for the standard transfer learning approach, where it can be especially attributed to the achievement of the highest accuracy (13.6 %, compared to the next best approach ANIL with 9.8 %) on the class legumes harvested green, which is the most abundant class in Estonia that is not shared with Latvia.

6.1.2. Impact of Portugal Pre-Training Data

Table 3b (**LV+PT**→**EE**) evaluates the results when pre-training on data from both Latvia and Portugal, followed by fine-tuning on Estonian data. The addition of Portugal to the pre-training data reveals interesting limitations when it comes to geographical knowledge transfer. The results indicate that none of the algorithms was able to overcome the discrepancies between Portuguese and Estonian data, which are inherent due to their

geographical locations. However, FOMAML showed improved Cohen’s kappa scores (highlighted in green). Moreover, the relative performance of, for instance, MAML compared to regular transfer learning improves with the addition of Portugal data, suggesting that increasing the formal dataset diversity can enhance certain aspects of the model’s performance. Table 4b (20-shot **LV+PT**→**EE**) shows once more that when evaluating on Estonia-specific classes ($EE \setminus (LV \cup PT)$), most meta-learning algorithms (except TIML with encoder) and conventional transfer learning demonstrate significantly superior accuracy compared to the baseline. Moreover, this time, all approaches are even more affected by the pasture meadow grassland grass class and show a significant loss in performance when not taking it into account ($(EE \cap LV \cap PT) \setminus (\text{pasture meadow grassland grass})$). However, apart from TIML (with encoder), they still show superiority compared to no pre-training, with MAML and FOMAML performing best.

6.2. Limitations of the TIML family

The algorithms of the TIML family, despite having incorporated additional parcel location information, show rather mediocre performance on our multi-class cross-regional benchmark. Although the original implementation (Tseng et al. (2022))

Table 4: Detailed analysis of the 20-shot benchmark tasks. The metric *classification accuracy* was evaluated on subsets of the test dataset corresponding to classes that are overlapping, overlapping excluding pasture meadow grassland grass, or non-overlapping (cf. Figure 3) between the countries for the best performing pre-training scenario (in terms of accuracy on the validation dataset) per algorithm. We report the mean \pm standard deviation over five repeated experimental runs in all cases. The best result per subset is marked in **bold**.

		EE [§]	EE \cap LV	(EE \cap LV) \setminus {meadow}	EE \setminus LV
accuracy	no pre-training	0.490 \pm 0.020	0.542 \pm 0.022	0.17 \pm 0.12	0.021 \pm 0.022
	transfer learning	0.365 \pm 0.081	0.39 \pm 0.10	0.33 \pm 0.11	0.15 \pm 0.12
	ANIL	0.490 \pm 0.069	0.536 \pm 0.077	0.364 \pm 0.064	0.069 \pm 0.014
	MAML	0.507 \pm 0.057	0.556 \pm 0.063	0.335 \pm 0.058	0.055 \pm 0.069
	FOMAML	0.476 \pm 0.039	0.500 \pm 0.090	0.205 \pm 0.097	0.020 \pm 0.022
	TIML (encoder)	0.423 \pm 0.067	0.465 \pm 0.078	0.178 \pm 0.040	0.045 \pm 0.037
	TIML (no encoder)	0.456 \pm 0.058	0.499 \pm 0.068	0.31 \pm 0.10	0.062 \pm 0.044

		EE [§]	EE \cap LV \cap PT	(EE \cap LV \cap PT) \setminus {meadow}	(EE \cap LV) \setminus PT	(EE \cap PT) \setminus LV	EE \setminus (LV \cup PT)
accuracy	no pre-training	0.490 \pm 0.020	0.648 \pm 0.042	0.079 \pm 0.077	0.24 \pm 0.15	0.016 \pm 0.015	0.046 \pm 0.058
	transfer learning	0.292 \pm 0.089	0.28 \pm 0.14	0.132 \pm 0.028	0.415 \pm 0.052	0.095 \pm 0.082	0.170 \pm 0.032
	ANIL	0.480 \pm 0.045	0.563 \pm 0.082	0.129 \pm 0.060	0.413 \pm 0.091	0.053 \pm 0.060	0.19 \pm 0.11
	MAML	0.452 \pm 0.094	0.51 \pm 0.14	0.147 \pm 0.044	0.44 \pm 0.10	0.035 \pm 0.029	0.20 \pm 0.11
	FOMAML	0.445 \pm 0.058	0.49 \pm 0.10	0.147 \pm 0.078	0.475 \pm 0.083	0.064 \pm 0.093	0.17 \pm 0.14
	TIML (encoder)	0.438 \pm 0.031	0.582 \pm 0.072	0.064 \pm 0.048	0.20 \pm 0.12	0.029 \pm 0.037	0.036 \pm 0.053
	TIML (no encoder)	0.441 \pm 0.070	0.48 \pm 0.11	0.119 \pm 0.036	0.494 \pm 0.056	0.047 \pm 0.036	0.221 \pm 0.071

successfully applied TIML on a binary classification task, our extension of applying it on a multi-class benchmark reveals significant challenges. The algorithms seem to be overly sensitive to geographical features, making them a persistent limitation throughout the training process. This might be attributed to several factors. The geographical transfer introduces an additional domain shift to the problem, which appears to be further amplified by adding the parcel’s locations. The model’s reliance on parcel-level location features can intensify these issues, in particular when integrating Portuguese parcel locations, as it struggles to generalize patterns that are too tied to the unique local conditions of the pre-training data. This appears to be especially an issue for the TIML encoder, which represents a learnable property in itself. The encoder’s architecture likely prioritizes capturing fine-grained, region-specific features at the expense of regional generalization. As a result, it risks overfitting to the training regions, particularly when faced with the additional variability introduced by cross-country data. This raises the question to what extent the encoder can effectively leverage the knowledge acquired from the pre-training on distant location information during fine-tuning. Likewise, adding static location data as features to temporally structured time series data, as implemented in TIML (without encoder), can obscure the inherent temporal patterns. However, a detailed individual analysis of the TIML encoder algorithm is beyond the scope of this article and will be left for future work. Moreover, with a rising number of shots, the marginal superiority of TIML (with encoder) in regard to Cohen’s kappa shifts to an inferiority. This indicates that in datasets with a significant class imbalance, the encoder is not explicitly oriented toward learning discriminative features between minority classes. Instead, it learns general features that do not capture the nuances of minority classes. The combination

of these factors—geographical domain shifts, feature granularity issues, and encoder architectural limitations—makes it difficult for TIML to effectively transfer knowledge across such heterogeneous datasets. In general, the geographical location might not be a strong predictor of different crop patterns, given that similar latitudes can show divergent agricultural practices.

6.3. Run-time analysis

Despite their superior performance, algorithms from the MAML and TIML families tend to require longer training periods and greater computational resources compared to baselines. While ANIL and FOMAML significantly reduce computational costs compared to the standard MAML algorithm, run-time remains one of their major drawbacks. Run-times of the meta-learning family are fairly stable across the two tasks with and without incorporating data from Portugal. In contrast, the run-times of baseline algorithms increase substantially when incorporating the additional data from Portugal. A detailed run-time analysis can be found in Table C.12 in Appendix C.

6.4. Summary of key findings

In light of the discrepancy between Portugal and the other two countries, it can be posited that the Portugal data do not positively contribute to the transfer learning task. Indeed, when pre-training solely on Latvian data, the meta-learning algorithms perform well. The results also show a strong bias towards the pasture meadow grassland grass class, suggesting that having such a dominant class in the dataset impedes the transfer learning of other crop classes. In summary, meta-learning algorithms like ANIL and (FO-)MAML generally outperform simple transfer learning, especially as the number of training shots increases. However, the main drawback of high training run-times persists.

The use of multiple data sources from different geographical regions (as evidenced in the LV+PT→EE tasks) results in a decrease in overall performance, indicating that the Portuguese data is too disparate to improve the efficacy of knowledge transfer. At least none of the investigated algorithms was able to effectively transfer relevant knowledge from very different regions.

There are several possible reasons why adding Portugal data may not lead to an improvement:

Climate Estonia and Latvia have similar climates, making it easier for the models to generalize between them. Portugal’s different Mediterranean climate disrupts this, resulting in a greater feature distribution shift. This can result in model bias and, hence, reduces the effectiveness of pre-training.

Crop diversity As visualized in Figure 3, Estonia and Latvia share more common crop types, while Portugal introduces classes not present in the Baltic states. This potentially leads to less effective knowledge transfer.

Agricultural practices Differences in crop management, such as irrigation and soil treatment, vary significantly between Portugal and the Baltic regions, making it difficult for models trained on one region to adapt to the other. The soils in Portugal are fairly arid, acidic, and rocky (Inácio et al., 2008) compared to the humid, sandy, or clay soils in Latvia (Karklins, 2002) and Estonia (Kmoch et al., 2021).

Growth cycle differences Different climates also mean different growth periods for certain similar crops, making it challenging for models to align temporal data between regions.

The TIML algorithm, while showing competitive accuracy with encoder, generally performs best when fewer training samples were available. Nevertheless, Cohen’s kappa for TIML (with encoder) indicates that the model is unable to discern the differences between various crop classes, instead demonstrating a proclivity for the majority class.

7. Conclusion

This study provides the first extensive benchmark of meta-learning algorithms, including MAML, FOMAML, ANIL, and TIML, applied to crop type classification across multiple countries using the EUROCRPSML dataset. The evaluation spans diverse European regions, offering new insights into the effectiveness of these methods for real-world remote sensing applications in agriculture. The results indicate that while meta-learning algorithms from the MAML family generally outperform transfer learning in terms of accuracy and Cohen’s kappa, they come with increased computational costs and training time. The TIML family of algorithms did not show a significant improvement in prediction accuracy. Incorporating additional data from a more distant geographical country into the pre-training stage did not lead to enhanced performance. This indicates that regional disparities may not be conducive to effective knowledge transfer and serves to illustrate the inherent difficulties associated with the transfer of knowledge between disparate geographical regions.

In general, the study demonstrates the complexity of applying meta-learning techniques to geospatial problems. Although meta-learning can adapt to variations within similar regions, transferring knowledge between regions with substantial differences requires careful consideration of the characteristics of the underlying data. These findings highlight the trade-offs between computational efficiency and prediction accuracy in machine learning applications for remote sensing and crop type classification. Hence, we encourage researchers to first investigate regular transfer learning approaches to establish a baseline for cross-country adaptation before exploring whether meta-learning techniques could improve classification performance.

Using the newly introduced EUROCRPSML dataset, this study sets a precedent for future benchmarks in agricultural remote sensing, providing a valuable resource to evaluate novel machine learning algorithms or models on real-world, multi-class and multi-region crop type data.

8. CRediT authorship contribution statement

J. Reuss: Conceptualization, Data curation, Formal analysis, Investigation, Methodology, Resources, Software, Validation, Visualization, Writing – original draft, Writing – review & editing. **J. Macdonald:** Conceptualization, Formal analysis, Investigation, Methodology, Resources, Software, Validation, Visualization, Writing – original draft, Writing – review & editing. **S. Becker:** Conceptualization, Formal analysis, Investigation, Validation, Visualization, Writing – original draft, Writing – review & editing. **K. Schultka:** Conceptualization, Methodology, Software. **L. Richter:** Conceptualization, Funding acquisition, Supervision, Writing – review & editing. **M. Körner:** Conceptualization, Funding acquisition, Project administration, Supervision, Writing – review & editing.

9. Declaration of competing interest

The authors declare that they have no known competing financial interests or personal relationships that could have appeared to influence the work reported in this paper.

10. Acknowledgments

The project is funded by the German Federal Ministry for Economics and Climate Action based on a decision by the German Bundestag under the funding reference 50EE2007B (J. Reuss and M. Körner), 50EE2007A (J. Macdonald, S. Becker, K. Schultka, and L. Richter) and 50EE2105 (M. Körner). S. Becker acknowledges support by SNF Grant PZ00P2 216019.

References

- Akiba, T., Sano, S., Yanase, T., Ohta, T., Koyama, M., 2019-07. Optuna: A next-generation hyperparameter optimization framework, in: 25th ACM SIGKDD International Conference on Knowledge Discovery and Data Mining, pp. 2623–2631. doi:[10.1145/3292500.3330701](https://doi.org/10.1145/3292500.3330701).

- Antonijević, O., Jelić, S., Bajat, B., Kilibarda, M., 2023. Transfer learning approach based on satellite image time series for the crop classification problem. *Journal of Big Data* 10, 54. doi:[10.1186/s40537-023-00735-2](#).
- Baik, S., Choi, M., Choi, J., Kim, H., Lee, K.M., 2020. Meta-learning with adaptive hyperparameters, in: *Advances in Neural Information Processing Systems (NeurIPS)*.
- Bekmukhamedov, N., Karabkina, N., Kurbanova, R., Koshim, G.A., Yegizbayeva, A., Ilyas, S., 2024-01-16. Advancing rice yield forecasting and crop assessment in kazakhstan's kyzylorda region, in: Slimani, K., Gerasymov, O., Kerkeb, M. (Eds.), *International Conference on Smart Technologies and Applied Research (STAR)*. doi:[10.1051/e3sconf/202447700001](#).
- Boussiou, L., Zeng, C., Guenais, T., Bertsimas, D., 2022. Hurricane forecasting: A novel multimodal machine learning framework. *Weather and Forecasting* 37. doi:[10.1175/WAF-D-21-0091.1](#).
- Dumoulin, V., Hounsby, N., Evci, U., Zhai, X., Goroshin, R., Gelly, S., Larochelle, H., Larochelle, H., 2021. A unified few-shot classification benchmark to compare transfer and meta learning approaches, in: Vanschoren, J., Yeung, S. (Eds.), *Neural Information Processing Systems Track on Datasets and Benchmarks*.
- Finn, C., Abbeel, P., Levine, S., 2017. Model-agnostic meta-learning for fast adaptation of deep networks, in: *34th International Conference on Machine Learning - Volume 70*, pp. 1126–1135. doi:[10.5555/3305381.3305498](#).
- Gokaslan, A., Cohen, V., Pavlick, E., Tellex, S., 2019. Openwebtext corpus. URL: <http://Skylion007.github.io/OpenWebTextCorpus>.
- Gómez, C., White, J.C., Wulder, M.A., 2016. Optical remotely sensed time series data for land cover classification: A review. *ISPRS Journal of Photogrammetry and Remote Sensing (P&RS)* 116, 55–72. doi:[10.1016/j.isprsjprs.2016.03.008](#).
- Hao, P., Di, L., Zhang, C., Guo, L., 2020. Transfer learning for crop classification with cropland data layer data (cdl) as training samples. *Science of The Total Environment* 733, 138869. doi:[10.1016/j.scitotenv.2020.138869](#).
- Hospedales, T., Antoniou, A., Micaelli, P., Storkey, A., 2022. Meta-learning in neural networks: A survey. *IEEE Transactions on Pattern Analysis and Machine Intelligence (TPAMI)* 44, 5149–5169. doi:[10.1109/TPAMI.2021.3079209](#).
- Huisman, M., van Rijn, J.N., Plaat, A., 2021. A survey of deep meta-learning. *Artificial Intelligence Review* 54, 4483–4541. doi:[10.1007/s10462-021-10004-4](#).
- Inácio, M., Pereira, V., Pinto, M., 2008. The soil geochemical atlas of portugal: Overview and applications. *Journal of Geochemical Exploration* 98, 22–33. doi:[10.1016/j.gexplo.2007.10.004](#).
- Karklins, A., 2002. A comparative study of the latvian soil classification with wrb, in: *Soil Classification 2001*. E. Micheli, F. O. Nachtergaele, R. J. A. Jones, L. Montanarella (eds). European Soil Bureau Research Report No. 7, EUR 20398 EN Luxembourg: Office for Official publications of the European Communities 17 World Congress of Soil Science, Bangkok, Thailand, pp. 199–204.
- Kerner, H.R., Tseng, G., Becker-Reshef, I., Nakalembe, C., Barker, B., Munshell, B., Paliyam, M., Hosseini, M., 2020. Rapid response crop maps in data sparse regions, in: *ACM SIGKDD Conference on Data Mining and Knowledge Discovery Workshops*. doi:[10.48550/arXiv:2006.16866](#).
- Kingma, D.P., Ba, J., 2017. Adam: A method for stochastic optimization, in: *International Conference on Learning Representations (ICLR)*. doi:[10.48550/arXiv:1412.6980](#).
- Kmoch, A., Kanak, A., Astover, A., Kull, A., Virro, H., Helm, A., Pärtel, M., Ostonen, I., Uuemaa, E., 2021. EstSoil-EH: A high-resolution eco-hydrological modelling parameters dataset for estonia. *Earth System Science Data* 13, 83–97. doi:[10.5194/essd-13-83-2021](#).
- Kumar, S., Torres, C., Ullat, O., Ayasse, A., Roberts, D., Manjunath, B., 2020. Deep remote sensing methods for methane detection in overhead hyperspectral imagery, in: *IEEE Winter Conference on Applications of Computer Vision (WACV)*, pp. 1765–1774. doi:[10.1109/WACV45572.2020.9093600](#).
- Lee, K., Maji, S., Ravichandran, A., Soatto, S., 2019. Meta-learning with differentiable convex optimization, in: *IEEE/CVF Conference on Computer Vision and Pattern Recognition (CVPR)*, pp. 10649–10657. doi:[10.1109/CVPR.2019.01091](#).
- Li, Z., Zhou, F., Chen, F., Li, H., 2017. Meta-sgd: Learning to learn quickly for few-shot learning doi:[10.48550/arXiv:1707.09835](#).
- Marković, M., Živaljević, B., Mimić, G., Woznicki, S., Marko, O., Lugonja, P., 2023. Using sentinel-1 data for soybean harvest detection in vojvodina province, serbia, in: Neale, C.M.U., Maltese, A. (Eds.), *Remote Sensing for Agriculture, Ecosystems, and Hydrology XXV*, p. 127271G. doi:[10.1117/12.2679417](#).
- Miranda, B., Yu, P., Goyal, S., Wang, Y.X., Koyejo, S., 2023. Is Pre-training Truly Better Than Meta-Learning?, in: *Proceedings of the 40th International Conference on Machine Learning 2023 DMLR Workshop*. doi:[10.48550/arXiv.2306.13841](#), [arXiv:2306.13841](#).
- Mishra, N., Rohaninejad, M., Chen, X., Abbeel, P., 2018. A simple neural attentive meta-learner, in: *International Conference on Learning Representations (ICLR)*, pp. 1–17.
- National Agricultural Statistics Service, 2024. National Agricultural Statistics Service Cropland Data Layer. Technical Report. United States Department of Agriculture (USDA). URL: https://www.nass.usda.gov/Research_and_Science/Cropland/SARS1a.php.
- Nichol, A., Achiam, J., Schulman, J., 2018. On first-order meta-learning algorithms. *CoRR abs/1803.02999*. URL: <http://arxiv.org/abs/1803.02999>, [arXiv:1803.02999](#).
- Odenweller, J.B., Johnson, K.I., 1984. Crop identification using landsat temporal-spectral profiles. *Remote Sensing of Environment* 14, 39–54. doi:[10.1016/0034-4257\(84\)90006-3](#).
- Paszke, A., Gross, S., Massa, F., Lerer, A., Bradbury, J., Chanan, G., Killeen, T., Lin, Z., Gimelshein, N., Antiga, L., Desmaison, A., Kopf, A., Yang, E., DeVito, Z., Raison, M., Tejani, A., Chilamkurthy, S., Steiner, B., Fang, L., Bai, J., Chintala, S., 2019. Pytorch: An imperative style, high-performance deep learning library, in: Wallach, H., Larochelle, H., Beygelzimer, A., d'Alché Buc, F., Fox, E., Garnett, R. (Eds.), *Advances in Neural Information Processing Systems (NeurIPS)*. [arXiv:2011.00209](#).

- Raghu, A., Raghu, M., Bengio, S., Vinyals, O., 2019-09-19. Rapid learning or feature reuse? [arXiv:1909.09157](#).
- Reed, B.C., Brown, J.F., VanderZee, D., Loveland, T.R., Merchant, J.W., Ohlen, D.O., 1994. Measuring phenological variability from satellite imagery. *Journal of Vegetation Science* 5, 703–714. doi:[10.2307/3235884](#).
- Reuss, J., Macdonald, J., 2024. Eurocropsml. doi:[10.5281/zenodo.15095445](#). [dataset].
- Reuss, J., Macdonald, J., Becker, S., Richter, L., Körner, M., 2025. Eurocropsml: A time series benchmark dataset for few-shot crop type classification. *Nature Scientific Data* [arXiv:2407.17458](#).
- Rußwurm, M., Pelletier, C., Zollner, M., Lefèvre, S., Körner, M., 2020. BreizhCrops: A time series dataset for crop type mapping, in: ISPRS – International Archives of the Photogrammetry, Remote Sensing and Spatial Information Sciences, pp. 1545–1551. doi:[10.5194/isprs-archives-XLIII-B2-2020-1545-2020](#).
- Rusu, A.A., Rao, D., Sygnowski, J., Vinyals, O., Pascanu, R., Osindero, S., Hadsell, R., 2018. Meta-learning with latent embedding optimization, in: International Conference on Learning Representations (ICLR). [arXiv:1807.05960](#).
- Rußwurm, M., Wang, S., Körner, M., Lobell, D., 2020. Meta-learning for few-shot land cover classification, in: IEEE/CVF Conference on Computer Vision and Pattern Recognition Workshops (CVPRW), p. 9. doi:[10.1109/cvprw50498.2020.00108](#).
- Sainte Fare Garnot, V., Landrieu, L., Giordano, S., Chehata, N., 2020. Satellite image time series classification with pixel-set encoders and temporal self-attention, in: IEEE/CVF Conference on Computer Vision and Pattern Recognition (CVPR), pp. 12322–12331. doi:[10.1109/CVPR42600.2020.01234](#).
- Santaga, F.S., Benincasa, P., Toscano, P., Antognelli, S., Ranieri, E., Vizzari, M., 2021. Simplified and advanced sentinel-2-based precision nitrogen management of wheat. *Agronomy* 11. doi:[10.3390/agronomy11061156](#).
- Santoro, A., Bartunov, S., Botvinick, M., Wierstra, D., Lillicrap, T., 2016-06. Meta-learning with memory-augmented neural networks, in: Balcan, M.F., Weinberger, K.Q. (Eds.), International Conference on Machine Learning (ICML), pp. 1842–1850.
- Schmitt, M., Ahmadi, S.A., Hänsch, R., 2021. There is no data like more data - current status of machine learning datasets in remote sensing, in: IEEE International Geoscience and Remote Sensing Symposium (IGARSS), pp. 1206–1209. doi:[10.1109/IGARSS47720.2021.9555129](#).
- Schneider, M., Broszeit, A., Körner, M., 2021. EuroCrops: A pan-european dataset for time series crop type classification, in: Soille, P., Loekken, S., Albani, S. (Eds.), Conference on Big Data from Space (BiDS), Publications Office of the European Union. p. 4. doi:[10.2760/125905](#).
- Schneider, M., Chan, A., Körner, M., 2023a. EuroCrops. doi:[10.5281/zenodo.10118572](#).
- Schneider, M., Körner, M., 2021. [re] satellite image time series classification with pixel-set encoders and temporal self-attention. *ReScience C* 7. doi:[10.5281/zenodo.4835356](#).
- Schneider, M., Schelte, T., Schmitz, F., Körner, M., 2023b. EuroCrops: The largest harmonized open crop dataset across the european union. *Nature Scientific Data* 10. doi:[10.1038/s41597-023-02517-0](#).
- Shankar, S., Halpern, Y., Breck, E., Atwood, J., Wilson, J., Sculley, D., 2017. No classification without representation: Assessing geodiversity issues in open data sets for the developing world, in: Advances in Neural Information Processing Systems (NIPS) Workshops, p. 5. [arXiv:1711.08536](#).
- Singh Behl, H., Güneş Baydin, A., Torr, P.H.S., 2019. Alpha MAML: Adaptive model-agnostic meta-learning, in: International Conference on Machine Learning (ICML) Workshops. [arXiv:1905.07435](#).
- Snell, J., Swersky, K., Zemel, R., 2017. Prototypical networks for few-shot learning, in: Guyon, I., Luxburg, U.V., Bengio, S., Wallach, H., Fergus, R., Vishwanathan, S., Garnett, R. (Eds.), Advances in Neural Information Processing Systems (NIPS), p. 13.
- Song, X.P., Hansen, M.C., Potapov, P., Adusei, B., Pickering, J., Adami, M., Lima, A., Zalles, V., Stehman, S.V., Di Bella, C.M., Conde, M.C., Copati, E.J., Fernandes, L.B., Hernandez-Serna, A., Jantz, S.M., Pickens, A.H., Turubanova, S., Tyukavina, A., 2021-06. Massive soybean expansion in south america since 2000 and implications for conservation. *Nature Sustainability* 2021, 784–792. doi:[10.1038/s41893-021-00729-z](#).
- Sung, F., Yang, Y., Zhang, L., Xiang, T., Torr, P.H., Hospedales, T.M., 2018. Learning to compare: Relation network for few-shot learning, in: IEEE Conference on Computer Vision and Pattern Recognition (CVPR), pp. 1199–1208. [arXiv:1711.06025](#).
- Thrun, S., Pratt, L., 1998. Learning to Learn: Introduction and Overview. Springer US. chapter 1. pp. 3–17. doi:[10.1007/978-1-4615-5529-2_1](#).
- Tian, Y., Wang, Y., Krishnan, D., Tenenbaum, J.B., Isola, P., 2020. Rethinking few-shot image classification: A good embedding is all you need?, in: European Conference on Computer Vision (ECCV), Springer. pp. 266–282. doi:[10.1007/978-3-030-58568-6_16](#).
- Triantafillou, E., Zhu, T., Dumoulin, V., Lamblin, P., Evci, U., Xu, K., Goroshin, R., Gelada, C., Swersky, K.J., Manzagol, P.A., Larochelle, H., 2020. Meta-dataset: A dataset of datasets for learning to learn from few examples, in: International Conference on Learning Representations (ICLR), p. 24. [arXiv:1903.03096](#).
- Tseng, G., Kerner, H., Rolnick, D., 2022. TIML: task-informed meta-learning for agriculture. *CoRR* abs/2202.02124. URL: <https://arxiv.org/abs/2202.02124>, doi:[10.48550/arXiv:2202.02124](#).
- Tseng, G., Zvonkov, I., Nakalembe, C., Kerner, H.R., 2021. CropHarvest: A global dataset for crop-type classification, in: Vanschoren, J., Yeung, S. (Eds.), Neural Information Processing Systems Track on Datasets and Benchmarks, p. 14.
- Tuia, D., Schindler, K., Demir, B., Zhu, X.X., Kochupillai, M., Džeroski, S., van Rijn, J.N., Hoos, H.H., Del Frate, F., Datcu, M., Markl, V., Le Saux, B., Schneider, R., Camps-Valls, G., 2025. Artificial intelligence to advance earth observation: a perspective. *IEEE Geoscience and Remote Sensing Magazine*, 2–25doi:[10.1109/mg-rs.2024.3425961](#).
- Turkoglu, M.O., D’Aronco, S., Perich, G., Liebis, F., Streit, C., Wegner, J.D., 2021. Crop mapping from image time series: Deep learning with multi-scale label hierarchies. *Remote Sensing of Environment* 264, 112603. doi:[10.1016/j.rse.2021.112603](#).

Vaswani, A., Shazeer, N., Parmar, N., Uszkoreit, J., Jones, L., Gomez, A.N., Kaiser, L., Polosukhin, I., 2017. Attention is all you need, in: Advances in Neural Information Processing Systems (NeurIPS). [arXiv:1706.03762](#).

Vinyals, O., Blundell, C., Lillicrap, T., Kavukcuoglu, K., Wierstra, D., 2016. Matching networks for one shot learning, in: Advances in Neural Information Processing Systems (NIPS). [arXiv:1806.03836](#).

Wang, A.X., Tran, C., Desai, N., Lobell, D., Ermon, S., 2018. Deep transfer learning for crop yield prediction with remote sensing data, in: ACM Conference on Computing and Sustainable Societies, pp. 1–5. doi:[10.1145/3209811.3212707](#).

Wang, S., Rußwurm, M., Körner, M., Lobell, D.B., 2020. Meta-learning for few-shot time series classification, in: IEEE International Geoscience and Remote Sensing Symposium (IGARSS), pp. 7041–7044. doi:[10.1109/IGARSS39084.2020.9441016](#).

Ye, H.J., Chao, W.L., 2021. How to train your maml to excel in few-shot classification, in: International Conference on Learning Representations (ICLR). [arXiv:2106.16245](#).

Yoon, J., Kim, T., Dia, O., Kim, S., Bengio, Y., Ahn, S., 2018. Bayesian model-agnostic meta-learning, in: Bengio, S., Wallach, H., Larochelle, H., Grauman, K., Cesa-Bianchi, N., Garnett, R. (Eds.), Advances in Neural Information Processing Systems (NeurIPS).

Appendix A. Implementation Details

We implement all algorithms within the PyTorch framework (Paszke et al., 2019) for machine learning and automatic differentiation.

Appendix A.1. Neural Network Architecture

For all experiments, we use a state-of-the-art Transformer encoder with four attention heads and one encoder layer, where each token in the input sequence is represented by an internal embedding vector of dimension 128. We apply additive sinusoidal positional encodings as introduced by Vaswani et al. (2017) to the input sequence, with a maximum sequence length of 366 days.¹ The hidden layer in the encoder’s feed-forward network has dimension 264.

We are considering a classification problem and directly apply a final linear classification layer on top of the Transformer encoder. There is no Transformer decoder part, as commonly used in generative approaches.

Appendix A.2. Model training

The general training follows the two-phase approach of pre-training and fine-tuning. Besides the actual learnable parameters of the Transformer model (weights), there are a number of non-learned hyperparameters that influence the model. These include hyperparameters that were manually/empirically selected (batch size for the mini-batch gradient descent, annealing schedules for

Table A.5: The hyperparameters employed during meta-learning, along with their corresponding valid values, were either set manually/empirically, or were automatically tuned.

[§] The encoder learning rate corresponds to the learning rate of the TIML encoder and, hence, was solely employed for the purpose of TIML (with encoder) training.

hyperparameter	value / value range	assignment
tuning tasks	100 000	manual
tuning trials per setup	36	manual
inner learning rate α	$\alpha \in [0.01, 10.0]$	tuned
outer learning rate β	$\beta \in [0.0001, 0.1]$	tuned
encoder learning rate η [§]	$\eta \in [0.0001, 0.1]$	tuned
training tasks	100 000	manual
number of tasks per batch	4	manual
number of classes per task n	$n \in \{4, 10\}$	empirical
number of samples per class k	$k \in \{1, 10\}$	empirical
number of inner loop gradient steps s	$s \in \{1, 4, 10\}$ for $n = 4$, $s = 1$ for $n = 10$	empirical

learning rates), as well as hyperparameters that were automatically tuned over numerous trial runs (learning rates). The term "empirically selected" denotes that experiments were conducted with a range of values for the respective hyperparameter, with the optimal value being determined on the basis of the validation accuracy. The manually set values, along with the valid ranges for tuned and empirically determined hyperparameters, were established on the basis of initial experiments, which showed the greatest improvements with these settings (cf. Tables A.5 to A.7). The following subsections each contain an overview of the (tuned/selected) hyperparameters. For the tuning trial runs we employ a *Bayesian Tree-Parzen estimator (TPE)* with percentile pruning within the Optuna framework (Akiba et al., 2019-07). We employ a total of 100 warm-up steps and keep the top 75th percentile of runs. In all cases, the selection of the best hyperparameters is based on the classification accuracy in the validation dataset. This is also used to determine the best pre-training epoch. Its model state is used to initialize the model backbone weights before fine-tuning. Finally, the best fine-tuning epoch is determined by the classification accuracy in the validation dataset of the fine-tuning task. Its model state is used to compute the final reported model accuracy on the test dataset from the fine-tuning task.

Appendix A.3. Meta-Learning

All meta-learning algorithms are trained using a mini-batch stochastic gradient descent in the inner optimization loop and the Adam optimizer (Kingma and Ba, 2017) in the outer optimization loop. The learning rates for the inner and outer optimization loop are individually tuned on 20 000 meta-train tasks, as described in Appendix A.2. We then meta-train the models on 100 000 meta-training tasks and validate after every 100 tasks on the meta-validation tasks (corresponding to epochs for regular training). The classification head layer is adapted to predict a vector in \mathbb{R}^{n_c} of n_c class logits that correspond to the distinct classes. The weights of the classification head layer are reset at the start of each new inner optimization loop to allow it to adapt to each new batch of tasks. As mentioned in Section 4.3, we carry out a series of experiments with different n -way k -shot-settings and inner loop steps s , cf. Table A.5. Subsequently, all meta-trained models undergo fine-tuning on the Estonia data.

¹ Even though we are only looking at data from 2021, setting the maximum length of the positional encoding to 366 (leap year) provides a more flexible approach for further use cases. For instance, it allows fine-tuning of models that were pre-trained on leap year data

Table A.6: The hyperparameters utilized during transfer learning, along with their corresponding valid values. They were either set manually or empirically, or alternatively, were automatically tuned.

hyperparameter	value / value range	assignment
tuning epochs	150	manual
tuning trials per setup	36	manual
training epochs	150	manual
early stopping patience k (epochs)	15	manual
batch size b	$b \in \{1, 4, 16, 32, 64, 128, 264\}$	empirical
learning rate α	$\alpha \in [0.0001, 0.01]$	tuned
cosine annealing cycles c	$c \in \{0, 1, 2\}$	empirical

Appendix A.4. Transfer learning

The regular transfer learning experiments are conducted using the Adam optimizer (Kingma and Ba, 2017) with a tuned learning rate (cf. Appendix A.2) and a batch size of 128. We train for a maximum of 150 epochs on the training set, validate after each epoch on the validation set, and stop the training in case the validation loss does not decrease for more than 15 epochs (early stopping). Hyperparameter tuning and training are performed with varying batch sizes $b \in \{4, 8, 16, 32, 64, 128, 264\}$. Based on the validation accuracy, the batch size 128 is selected for further experimentation and subsequent fine-tuning. Hence, with a batch size of 128, we performed a series of experiments with the cosine annealing learning rate schedule. The number of cycles is set to zero (corresponding to no cosine annealing), one, or two cycles. We choose the most promising schedule based on the validation accuracy, which is one annealing cycle when pre-training only on data from Latvia, and no annealing when pre-training on data from Latvia and Portugal. Table A.6 contains an overview of all hyperparameters used during transfer learning.

Appendix A.5. Fine-tuning

For the meta-learned and pre-trained models, we reset the classification head layer before fine-tuning them on the fine-tuning task. All models are fine-tuned for a maximum of 200 epochs on Estonia tasks using an Adam optimizer (Kingma and Ba, 2017). We validate every epoch on the validation set. Training is stopped if the validation loss does not decrease for more than five epochs (early stopping). Furthermore, we adjust the learning rate(s) in three different settings as described in Appendix A.2:

1. We use the same learning rate for both the model backbone and the classification head.
2. We allow for different learning rates for the model backbone and the classification head.
3. We only allow for an adaptation of the classification head with a tuned learning rate and fix the model backbone learning rate to zero. This is equivalent to freezing the model backbone parameters.

Tables B.8 and B.9 illustrate the results of the 20-shot task, exemplifying the impact of the above learning rate settings. All experiments are repeated five times with five different random seeds $r \in \{0, 1, 42, 123, 1234\}$. We set the random seed across

multiple libraries, including Python’s built-in random module, NumPy’s random number generator, and PyTorch’s CPU random number generator. Moreover, we mandate that PyTorch utilizes deterministic algorithms for operations on the GPU when using CuDNN, and disable the auto-tuning functionality of CuDNN. Hence, for each random seed r , the experiments are almost entirely deterministic. The only remaining randomness is introduced by Optuna’s TPE during hyperparameter tuning. An overview of the relevant hyperparameters is shown in Table A.7.

Appendix B. Additional results

While Table 3a and Table 3b show only the best results for each algorithm and the fine-tuning task, we now provide a more detailed analysis of the different variants of the algorithm taking into account the three hyperparameter tuning scenarios of the learning rate (only head, different head & backbone, same head & backbone) as well as the different n -way k -shot s -step settings of the meta-learning algorithms.

Table B.8 (LV→EE) and Table B.9 (LV+PT→EE) show the classification accuracy of the 20-shot benchmarking tasks for the three learning rate tuning settings. Fine-tuning both the model backbone and the model head achieved higher prediction accuracies compared to only fine-tuning the model head in all cases. In addition, the most flexible setting with separately tuned learning rates for the model backbone and head performed best in the majority of cases. Noteworthy, the ANIL algorithm, which only adapts the learnable parameters of the model head during its inner optimization loop, did not perform better than the other transfer meta-learning approaches when fine-tuning only the model head. While in theory using just one learning rate is less flexible than allowing separate ones for head and backbone, using just one might still turn out to be advantageous: If the backbone and head use different learning rates, the gradient updates may vary significantly between the two, leading to an imbalance in how quickly each part adapts during training. This can cause the model to optimize one part faster than the other, potentially leading to suboptimal representations in the backbone or overfitting in the head.

Table B.10 (LV→EE) and Table B.11 (LV+PT→EE) show the classification accuracy of the 20-shot benchmarking tasks for the six n -way k -shot s -step settings of the meta-learning algorithms. Although there was no single setting that performed best in all algorithms and benchmark tasks, in most cases the best prediction accuracies could be achieved for meta-learning in 4-way 1-shot 4-step. This shows that all meta-learning algorithms could take advantage of taking more than one gradient step during the inner optimization for the task adaptation, but a small number of steps is sufficient. Furthermore, allowing for a larger number of classes ($n = 10$) and, thus, potentially a higher diversity between classes in tasks during pre-training did not improve downstream fine-tuning performance for any algorithm. Similarly, presenting the models with more samples per class ($k = 10$) and, thus, potentially a higher intraclass diversity in the tasks during pre-training also did not improve their fine-tuning performance in all but one case.

Table A.7: The hyperparameters utilized during fine-tuning, along with their corresponding valid values. Their final value was either assigned manually or empirically, or alternatively, was automatically tuned. The optimal batch size for fine-tuning, denoted by b , was identified through a process of fine-tuning the transfer learning models with varying fine-tuning batch sizes. Subsequently, the final batch size of 16 was selected based on the validation accuracy observed during the fine-tuning process.

lr tuning hyperparameter	only head value / value range	different head & backbone value / value range	same head & backbone value / value range	assignment
tuning epochs	200	200	200	manual
tuning trials per setup	8	32	8	manual
training epochs	200	200	200	manual
early stopping patience k (epochs)	5	5	5	manual
batch size b	16	16	16	empirical
learning rate α	$\alpha_{\text{head}} \in [10^{-6}, 10^{-2}]$, $\alpha_{\text{backbone}} = 0$	$\alpha_{\text{head}} \in [10^{-6}, 10^{-2}]$, $\alpha_{\text{backbone}} \in [10^{-6}, 10^{-3}]$	$\alpha \in [10^{-6}, 10^{-2}]$	tuned

Table B.8: Detailed analysis of the 20-shot **LV**→**EE** benchmark task. The metric *classification accuracy* was evaluated for three different learning rate tuning variants per algorithm. We report the mean \pm standard deviation over five repeated experimental runs in all cases. The best result per algorithm is marked in **bold**.

‡ The results of the baseline algorithm with no pre-training are independent of the benchmark scenario and thus identical in Table B.8 and Table B.9.

	lr tuning algorithm	only head	different head & backbone	same head & backbone
accuracy	no pre-training‡	0.32 \pm 0.18	0.486 \pm 0.017	0.463 \pm 0.035
	transfer learning	0.261 \pm 0.082	0.325 \pm 0.087	0.353 \pm 0.085
	ANIL	0.373 \pm 0.051	0.478 \pm 0.064	0.445 \pm 0.056
	MAML	0.386 \pm 0.056	0.493 \pm 0.058	0.463 \pm 0.072
	FOMAML	0.420 \pm 0.041	0.466 \pm 0.022	0.451 \pm 0.066
	TIML (encoder)	0.345 \pm 0.083	0.402 \pm 0.074	0.421 \pm 0.064
	TIML (no encoder)	0.378 \pm 0.080	0.448 \pm 0.062	0.423 \pm 0.067

Table B.9: Detailed analysis of the 20-shot **LV+PT**→**EE** benchmark task. The metric *classification accuracy* was evaluated for three different learning rate tuning variants per algorithm. We report the mean \pm standard deviation over five repeated experimental runs in all cases. The best result per algorithm is marked in **bold**.

‡ The results of the baseline algorithm with no pre-training are independent of the benchmark scenario and thus identical in Table B.8 and Table B.9.

	lr tuning algorithm	only head	different head & backbone diff	same head & backbone
accuracy	no pre-training‡	0.32 \pm 0.18	0.486 \pm 0.017	0.463 \pm 0.035
	transfer learning	0.171 \pm 0.021	0.256 \pm 0.071	0.261 \pm 0.095
	ANIL	0.365 \pm 0.060	0.470 \pm 0.056	0.406 \pm 0.084
	MAML	0.387 \pm 0.073	0.41 \pm 0.10	0.444 \pm 0.097
	FOMAML	0.377 \pm 0.096	0.440 \pm 0.058	0.420 \pm 0.058
	TIML (encoder)	0.343 \pm 0.024	0.397 \pm 0.039	0.418 \pm 0.049
	TIML (no encoder)	0.352 \pm 0.041	0.439 \pm 0.059	0.439 \pm 0.067

Table B.10: Detailed analysis of the 20-shot **LV**→**EE** benchmark task. The metric *classification accuracy* was evaluated for six different n -way k -shot s -step meta-learning variants per algorithm. We report the mean \pm standard deviation over five repeated experimental runs in all cases. The best result per algorithm is marked in **bold**.

	n -way	4	4	4	4	10	10
	k -shot	1	1	1	10	1	10
	s -step	1	4	10	1	1	1
	algorithm						
accuracy	ANIL	0.405 \pm 0.061	0.473 \pm 0.068	0.439 \pm 0.065	0.369 \pm 0.083	0.403 \pm 0.094	0.359 \pm 0.072
	MAML	0.464 \pm 0.060	0.465 \pm 0.067	0.419 \pm 0.041	0.417 \pm 0.084	0.361 \pm 0.078	0.463 \pm 0.058
	FOMAML	0.449 \pm 0.030	0.448 \pm 0.060	0.403 \pm 0.052	0.399 \pm 0.045	0.436 \pm 0.048	0.36 \pm 0.10
	TIML (encoder)	0.414 \pm 0.055	0.367 \pm 0.062	0.372 \pm 0.074	0.327 \pm 0.090	0.376 \pm 0.085	0.296 \pm 0.061
	TIML (no encoder)	0.385 \pm 0.063	0.391 \pm 0.073	0.433 \pm 0.081	0.379 \pm 0.077	0.371 \pm 0.050	0.340 \pm 0.064

Table B.11: Detailed analysis of the 20-shot **LV+PT**→**EE** benchmark task. The metric *classification accuracy* was evaluated for six different n -way k -shot s -step meta-learning variants per algorithm. We report the mean \pm standard deviation over five repeated experimental runs in all cases. The best result per algorithm is marked in **bold**.

	n -way	4	4	4	4	10	10
	k -shot	1	1	1	10	1	10
	s -step	1	4	10	1	1	1
	algorithm						
accuracy	ANIL	0.355 \pm 0.060	0.396 \pm 0.068	0.377 \pm 0.075	0.462 \pm 0.069	0.374 \pm 0.084	0.331 \pm 0.050
	MAML	0.379 \pm 0.073	0.44 \pm 0.11	0.347 \pm 0.076	0.362 \pm 0.081	0.388 \pm 0.063	0.357 \pm 0.037
	FOMAML	0.408 \pm 0.051	0.410 \pm 0.074	0.332 \pm 0.092	0.392 \pm 0.069	0.378 \pm 0.083	0.342 \pm 0.051
	TIML (encoder)	0.342 \pm 0.093	0.319 \pm 0.040	0.352 \pm 0.078	0.375 \pm 0.047	0.394 \pm 0.062	0.366 \pm 0.060
	TIML (no encoder)	0.361 \pm 0.030	0.424 \pm 0.048	0.418 \pm 0.094	0.314 \pm 0.052	0.314 \pm 0.059	0.356 \pm 0.053

Table C.12: Run-time for the considered algorithms during the pre-training and 500-shot fine-tuning phases per run of the model training. For the meta-learning algorithms we used the 4-way 1-shot 4-step variant. For the pre-training and fine-tuning, we report the run-time of the training phase, excluding the tuning. The fastest run-time per training phase is marked in **bold**.

benchmark task	LV→EE	LV→EE	LV+PT→EE	LV+PT→EE
training phase	pre-training	fine-tuning	pre-training	fine-tuning
algorithm / runtime	(in hours)	(in minutes)	(in hours)	(in minutes)
no pre-training	n/a	3.8 ± 1.9	n/a	11.7 ± 2.9
transfer learning	0.73	4.0 ± 1.2	2.9	10 ± 13
ANIL	3.8	5.8 ± 2.3	3.9	7.4 ± 3.0
MAML	5.3	5.1 ± 2.8	5.3	5.9 ± 2.4
FOMAML	4.1	7.4 ± 2.4	4.2	8.3 ± 7.5
TIML (encoder)	4.3	10.0 ± 3.5	4.3	19.9 ± 9.9
TIML (no encoder)	5.4	4.5 ± 1.9	5.7	17 ± 12

Appendix C. Run-time analysis

Besides performance measures such as prediction accuracy, computational costs and training times required to achieve performance are also of interest when benchmarking algorithms for their knowledge transfer capabilities. A complete and fully comparable run-time evaluation of all experiments considered in our benchmark is not possible since the experimental runs were partly run in parallel on multiple machines with varying hardware specifications. Instead, we present a run-time analysis of one algorithm pre-training variant per algorithm and one fine-tuning task. All of these were performed under comparable circumstances on the same machine with 16 cores of AMD® EPYC™ 9654 CPU, 64 GB RAM, and an NVIDIA® GeForce RTX™ 4090 GPU.

Table C.12 shows the model training times per algorithm during the pre-training and 500-shot fine-tuning. For meta-learning algorithms, we report the times of the 4-way 1-shot 4-step variant.

The randomly initialized benchmark model has the shortest overall training time, hence requiring no pre-training at all, as well as having the lowest fine-tuning times. While meta-learning algorithms of the MAML family fulfill the promise of quicker task adaptation and, thus, in general, good fine-tuning times, this comes at significantly increased computational costs during pre-training. Altogether, the meta-learning approaches require longer total training times, with TIML (without encoder) being the most compute-heavy of all compared algorithms. Interestingly, the run-times of the meta-learning algorithms are less affected by incorporating additional pre-training data from Portugal, while transfer learning takes significantly longer in this case. After pre-training also on Portugal data, for the fine-tuning phase, the MAML family performs best.